MECP2 in neuronal development in terms of neuronal stem cells, neuronal and glial cell differentiation during all developmental stages, the function of differentiated dopaminergic neurons, and the maturation of neuronal cells. All these results should prove useful for understanding not only the biological roles of MECP2 but also the pathogenesis of RTT. Recently, we also developed an iPS cell system that may provide a novel strategy for developmental analysis at the molecular and cellular levels.

7. Conclusion

Finally, we should consider the potential for future mouse studies on MECP2-null mutation using ES cells and iPS cells and discuss the future perspectives for the treatment and management of this disease.

The reversal of early lethality and of some neurological abnormalities in MECP2-/Y mice through the postnatal supply of normal MECP2 has raised hopes for an effective treatment [54]. To this end, we should continue to explore new therapeutic modalities, including ghrelin, BDNF [32], and other factors [35].

Acknowledgements

This study was partly supported by a Grant on Research on Psychiatric and Neurological Diseases and Mental Health (#19-8), a Grant from the Research Project for Overcoming Intractable Diseases (#21-Nan-chi-ippan-110) and a Grant on Research on Learning Disorders (#19-6) from the Ministry of Health, Labour and Welfare of Japan, and was also partly supported by a Grant-in-Aid for Scientific Research C (#18591172) from the Ministry of Education, Culture, Sports, Science and Technology (MEXT) of Japan.

We are grateful to Drs. Ken-ichiro Kosai, Yasunori Okabe, Yoshihiro Nishi, Munetsugu Hara, Jyunko Yoh, and Yasuyuki Kojima for their contribution. Finally, we would like to acknowledge the patients and the family members of the Rett Syndrome Association (Sakuranbo-kai). This manuscript was presented as a presidential report of the 52nd Annual Meeting of the Japanese Society of Child Neurology (in Japanese) which had been held on May 20–22, 2010, Fukuoka Japan.

References

[1] The Rett Syndrome Diagnostic Criteria Work Group. Diagnostic criteria for Rett syndrome. Ann Neurol 1988;23:425–8.
[2] Kerr AM, Nomura Y, Armstrong D, Anvret M, Belichenko PV, Budden S, et al. Guidelines for reporting clinical features in cases with MECP2 mutations. Brain Dev 2001;23:208–11.
[3] Hagberg B, Hanefeld F, Percy A, Skjeldal O. An update clinically appreciable diagnostic criteria in Rett syndrome. Comments to Rett syndrome clinical criteria consensus panel satellite to European Pediatric Neurology Society Meeting, 11 September 2001, Germany: Baden Baden, Eur J Pediatr Neurol 2002; 6: 1–5.
[4] Chahrour M, Zoghbi HY. The story of Rett syndrome: from clinic to neurobiology. Neuron 2007;56:422–37.
[5] Amir RE, Van den Veyver IB, Wan M, Tran CQ, Francke U, Zoghbi HY. Rett syndrome is caused by mutations in X-linked MECP2, encoding methyl-CpG-binding protein 2. Nat Genet 1999;23:185–8.
[6] Bienvenu T, Chelly J. Molecular genetics of Rett syndrome: when DNA methylation goes unrecognized. Nat Rev Genet 2006;7:415–26.
[7] Franke U. Rett syndrome and MECP2-status of knowledge 10 years after the genes. Invited speaker of Segawa program. No to Hattatsu 2010;42:S88.
[8] Nomura Y, Honda K, Segawa M. Pathophysiology of Rett syndrome. Brain Dev 1987;9:506–13.
[9] Segawa M, Nomura Y. Polysomnography in the Rett syndrome. Brain Dev 1992;14:S46–54.
[10] Zoghbi H, Milstien H, Butler IJ, Smith OB, Kaufman S, Glaze DG, et al. Cerebrospinal fluid biogenic amines and biopterin in Rett syndrome. Ann Neurol 1989;25:56–60.
[11] Perry TL, Dunn HG, Ho H-H, Crichton JU. Cerebrospinal fluid values for monoamine metabolites, gamma aminobutyric acid, and other amino compounds in Rett syndrome. J Pediatr 1988;112:234–8.
[12] Samaco RC, Mandel-Brehm C, Chao H-T, Ward CS, Fyffe-Maricich SL, Ren J, et al. Loss of MeCP2 in aminergic neurons causes cell-autonomous defects in neurotransmitter synthesis and specific behavioral abnormalities. PNAS 2009;106:21966–71.
[13] Lekman A, Witt-Engerstrom I, Gottfries J, Hagberg B, Percy AK, Svennerholm L. Rett syndrome: biogenic amines and metabolites in postmortem brain. Pediatr Neurol 1989;5:357–62.
[14] Ide S, Itoh M, Goto Y. Defect in normal developmental increase of the brain biogenic amine concentrations in the mecp2-null mouse. Neurosci Lett 2005;386:14–7.
[15] Wenk GL. Alteration in dopaminergic function in Rett syndrome. Neuropediatrics 1995;26:123–5.
[16] Kitt CA, Troncoso JC, Price DL, Naidu S, Moser H. Pathological changes in substantia nigra and basal forebrain neurons in Rett syndrome. Ann Neurol 1990;28:416–7.
[17] Satoi M, Matsuishi T, Yamada S, Yamashita Y, Ohtaki E, Mori K, et al. Decreased cerebrospinal fluid levels of β-phenylethylamine in patients with Rett syndrome. Ann Neurol 2000;47:801–3.
[18] Zhou G, Shoji H, Yamada S, Matsuishi T. Decreased cerebrospinal fluid β-phenylethylamine in Parkinson's disease. J Neurol Neurosurg Psychiatry 1997;63:754–8.
[19] Myer EC, Tripathi HL, Dewey WL. Hyperendorphinism in Rett syndrome: cause or result? Ann Neurol 1988;24:340–1.
[20] Budden SS, Myer EC, Buttler IJ. Cerebrospinal fluid studies in the Rett syndrome: biogenic amines and beta endorphins. Brain Dev 1990;12:81–4.
[21] Matsuishi T, Nagamitsu S, Yamashita Y, Murakami Y, Kimura A, Sakai T, et al. Decreased cerebrospinal fluid levels of substance P in patients with Rett syndrome. Ann Neurol 1997;42:978–81.
[22] Mai JK, Stephens PH, Hope A, Cuello AC. Substance P in the human brain. Neuroscience 1986;17:709–39.
[23] Hender J, Hender T, Wessberg P, Jonason J. Interaction of substance P with respiratory control system in the rat. J Pharmacol Exp Ther 1983;228:196–201.
[24] Deguchi K, Antalffy BA, Twohill LJ, Chakraborty S, Glaze DG, Armstrong DD. Substance P immunoreactivity in Rett syndrome. Pediatr Neurol 2000;22:259–66.
[25] Whitty CJ, Kapatos G, Bannon MJ. Neurotrophic effects of substance P on hippocampal neurons in vitro. Neurosci Lett 1993;164:141–4.

Please cite this article in press as: Matsuishi T et al. Rett syndrome: The state of clinical and basic research, and future perspectives.. Brain Dev

[26] McArthur AJ, Budden SS. Sleep dysfunction in Rett syndrome: a trial of exogenous melatonin treatment. Dev Med Child Neurol 1998;40:186–92.
[27] Miyamoto A, Oki J, Takahashi S, Okuno A. Serum melatonin kinetics and long-term melatonin treatment for sleep disturbance in Rett syndrome. Brain Dev 1999;21:59–62.
[28] Yamashita Y, Matsuishi T, Murakami Y, Kato H. Sleep disorder in Rett syndrome and melatonin treatment. Brain Dev 1999;21:570.
[29] Lappalainen R, Lindholm D, Riikonen R. Low levels of nerve growth factor in cerebrospinal fluid of children with Rett syndrome. J Child Neurol 1996;11:296–300.
[30] Chen WG, Chang Q, Lin Y, Meissner A, West AE, Griffith EC, et al. Derepression of BDNF transcription involves calcium-dependent phosphorylation of MeCP2. Science 2003;302:885–9.
[31] Martinowich K, Hattori D, Wu H, Fouse S, He F, Hu Y, et al. DNA methylation-related chromatin remodeling in activity-dependent BDNF gene regulation. Science 2003;302:890–3.
[32] Chang Q, Khare G, Dani V, Nelson S, Jaenisch R. The disease progression of Mecp2 mutant mice is affected by the level of BDNF expression. Neuron 2006;49:341–8.
[33] Larimore JL, Chapleau CA, Kudo S, Theibert A, Percy AK, Pozzo-Miller L. Bdnf overexpression in hippocampal neurons prevents dendritic atrophy caused by Rett-associated MECP2 mutations. Neurobiol Dis 2009;34:199–211.
[34] Itoh M, Ide S, Takashima S, Kudo S, Nomura Y, Segawa M, et al. Methyl CpG-binding protein 2 (a mutation of which causes Rett syndrome) directly regulates insulin-like growth factor binding protein 3 in mouse and human brains. J Neuropathol Exp Neurol 2007;66:117–23.
[35] Tropea D, Giacometti E, Wilson NR, Beard C, McCurry C, Fu DD, et al. Partial reversal of Rett syndrome-like symptoms in MeCP2 mutant mice. Proc Natl Acad Sci USA 2009;106:2029–34.
[36] Blue ME, Naidu S, Johnston MV. Development of amino acid receptors in frontal cortex from girls with Rett syndrome. Ann Neurol 1999;45:541–5.
[37] Hamberger A, Gillberg C, Palm A, Hagberg B. Elevated CSF glutamate in Rett syndrome. Neuropediatrics 1992;23:212–3.
[38] Yamashita Y, Matsuishi T, Ishibashi M, Kimura A, Onishi Y, Yonekura Y, et al. Decrease in benzodiazepine receptor binding in the brain of adult Rett syndrome. J Neurol Sci 1998;154:146–50.
[39] Haas RH, Rice MA, Trauner DA, Meritt A. Ketogenic diet in Rett syndrome. Am J Med Genet 1986;24(Suppl 1):5225–46.
[40] Wakai S, Kameda K, Ishikawa YI, Miyamoto S, Nagaoka M, Okabe M, et al. Rett syndrome: findings suggesting axonopathy and mitochondrial abnormalities. Pediatr Neurol 1990;6:164–6.
[41] Matsuishi T, Urabe F, Komori H, Yamashita Y, Naito E, Kuroda Y, et al. The Rett syndrome and CSF lactic patterns. Brain Dev 1992;14:68–70.
[42] Matsuishi T, Urabe F, Percy AK, Komori H, Yamashita Y, Schultz RS, et al. Kato H Abnormal carbohydrate metabolism in cerebrospinal fluid in Rett syndrome. J Child Neurol 1994;9: 26–30.
[43] Murakami Y, Yamashita Y, Matsuish T, Iwanaga R, Kato H. Cerebral oxygenation and hemodynamics during hyperventilation and sleep in patients with Rett syndrome. Brain Dev; 20: 574–578.
[44] Armstrong DD. Rett syndrome neuropathology review 2000. Brain Dev 2001;23:S72–6.
[45] Saito Y, Ito M, Ozawa Y, Matsuishi T, Hamano K, Takashima S. Reduced expression of neuropeptides can be related to respiratory disturbances in Rett syndrome. Brain Dev 2001;23:S122–6.
[46] Amir RE, Van den Veyver IB, Schultz R, Malicki DM, Tran CQ, Dahle EJ, et al. Influence of mutation type and X chromosome inactivation on Rett syndrome phenotypes. Ann Neurol 2000;47:670–9.
[47] Nan X, Bird A. The biological function of the methyl-CpG binding protein MECP2 and its implication in Rett syndrome. Brain Dev 2001;23:S32–7.
[48] Obata K, Matsuishi T, Yamashita Y, Fukuda T, Kuwajima K, Horiuchi I, et al. Mutation analysis of the Methyl-CpG binding protein 2 gene (MECP2) in patients with Rett syndrome. J Med Genet 2000;37:608–10.
[49] Fukuda T, Yamashita Y, Nagamitsu S, Miyamoto K, Jin JJ, Ohmori I, et al. Methyl-CpG binding protein 2 gene (MECP2) variations in Japanese patients with Rett syndrome: pathological mutations and polymorphisms. Brain Dev 2005;27:211–7.
[50] Yamashita Y, Kondo I, Fukuda T, Morishima R, Kusaga A, Iwanaga R, et al. Mutation analysis of the methyl-CpG-binding protein 2 gene (MECP2) in Rett patients with preserved speech. Brain Dev 2001;23:S157–60.
[51] Matsuishi T, Yamashita Y, Kusaga A. Neurobiology and neurochemistry of Rett syndrome. Brain Dev 2001;23:S58–61.
[52] Yoshihara F, Kojima M, Hosoda H, Nakazato M, Kangawa K. Ghrelin: a novel peptide for growth hormone release and feeding regulation. Curr Opin Nutr Metab Care 2002;5:391–5.
[53] Okabe Y, Kusaga A, Takahashi T, Mitsumasu C, Murai Y, Tanaka E, et al. Neural development of methyl-CpG-Binding protein 2-null embryonic stem cells: a system for studying Rett syndrome. Brain Res 2010 in press.
[54] Guy J, Gan J, Selfridge J, Cobb S, Bird A. Reversal of neurological defects in a mouse model of Rett syndrome. Science 2007;315:1143–7.

Please cite this article in press as: Matsuishi T et al. Rett syndrome: The state of clinical and basic research, and future perspectives.. Brain Dev

Rett Syndrome

Yoshiko Nomura, Segawa Neurological Clinic for Children, Tokyo, Japan

Definition and History

Rett syndrome (RS, RTT; MIM 312750) is a neurodevelopmental disorder caused by a mutation in the gene methyl-CpG-binding protein 2 gene (*MECP2*) encoding for methyl-CpG-binding protein2 (MeCP2).

Since the first clinical delineation, substantial progress has been achieved in the clinical understanding of RS, which has been further fortified by the finding of the causative gene.

Its clinical features consist of autistic symptomatology, mental retardation, stereotyped movements mainly involving hands and mouth, dystonia, scoliosis, epilepsy, abnormal respiratory patterns, acquired microcephalus, and female preponderance.

In RS, particular signs and symptoms appear in an age-dependent fashion and this is considered to be due to abnormal synaptogenesis at certain stages of the course of development caused by the *MECP2* mutation. The exploration of the role of *MECP2* in RS is helpful in understanding not only other developmental disorders but also normal brain development.

In 1966, Andreas Rett, a pediatrician in Vienna Austria, described a disorder with the specific symptoms occurring only in females as 'Über ein eigenertiges hirnatrophisches Syndriome bei Hyperammonämie' in German. In 1977, Rett wrote a chapter in the Handbook of Clinical Neurology entitled 'Cerebral Atrophy associated with hyperammonaemia'. Because his initial paper was written in German and his initial English paper was under the misleading heading of hyperammonemia, his original contribution had remained unknown outside of Austria and Germany. The clinical characteristics of the disorder were described as 'hyperammonaemia, hypomimia or amimia, alalia, stereotyped movement patterns in arms and hands, enhanced reflex activity, spastic increase in tone, gait apraxia, tendency to cerebral convulsive attacks, high grade of mental retardation, gynecotrophy (only females), and progressive course'. In 1972, this disorder was first described as 'Rett Syndrom' by Leiber in a syndrome textbook 'Die klinischen Syndrom' known in German-speaking area. In 1978, Ishikawa et al. wrote a short case report with identical symptoms and signs to the cases reported in the article by Rett; however, this report by Ishikawa was not noticed either. In 1983, the paper by Bengt Hagberg et al. in Annals of Neurlogy brought the disorder into medical nosology. We proposed for the first time, in 1984, that this disorder is a developmental disorder involving monoamine systems. In April 8, 1983, Rett organized the first meeting on this disorder in Vienna. It was only then that the international collaboration on the research of the disorder began intensively.

In 1999, the causative gene *MECP2* was identified by Amir et al., and the new era started on the clinical–biological–molecular correlation, and basic research of *MECP2* and its role in the development of brain began.

Pathogenesis/Pathophysiology

RS is associated with characteristic and complex phenotypes. The natural course of RS consists of a unique age-dependent appearance of the specific clinical symptoms and signs. The age-dependent presentation of the features of the disorder is important in considering its pathophysiology, because it reflects the changes taking place along the maturation of the responsible neurons or neuronal systems.

The onset of the disorder is in early infancy, although the initial symptoms and signs are very subtle. The early motor signs of RS are hypotonia with failure of crawling, abnormal pattern of walking, and disturbance in skillful hand manipulation. Clinical evaluation has revealed that the former results from postural hypotonia, with failure in locomotion. Additionally, neurophysiological examination has showed this to be due to hypofunction of the aminergic neurons of the brainstem. The latter signs are considered to indicate dysfunction of the corticospinal tract at higher levels.

Early psychobehavioral characteristics are a poor response to environmental stimulation, a poor formation of circadian rhythm, and more sleep during daytime, which are the earliest features of autistic tendency and can be speculated as being due to hypofunction of braistem serotonergic and noradrenergic systems.

Along with these features, the deceleration of head growth begins to appear in late infancy. This is speculated to be due to the dysfunction of noradrenergic neurons, which is involved in the cerebral cortical synaptogenesis.

The pathognomonic stereotyped hand movements appear in early childhood after the loss of purposeful hand use. These occur on the background of dystonic posturing and fixed position of the hands. With age, rigid hypertonia appears and later, fixed dystonic posture.

Encyclopedia of Movement Disorders (2010), vol. 3, pp. 38-41

The frequency of the repetitive hand movements has been found to be minimally affected by environmental manipulations, suggesting that the movements are driven by automatic reinforcement or neurochemical processes.

The pathophysiology of the stereotyped hand movements with the loss of purposeful hand use and appearance of dystonic posturing are thought to be induced by the dysfunction of the basal ganglia-premotor and supplementary motor area with dopaminergic receptor supersensitivity. Scoliosis, which manifests itself in early childhood and shows progression with time, is also considered to be part of the dystonia.

The psychobehavioral characteristics of the disease include autistic features, and sudden episodes of screaming, laughing, or crying. Abnormal sleep–wake rhythms are present from early infancy.

With regard to the abnormal respiratory patterns and suggested abnormal cardiorespiratory centers in the brainstem, the involvement of the brainstem serotonergic system has been proposed. It is also suggested from experimental observations in mice that decreased substance P and other neuromodulators in the brainstem are the cause of the abnormal respiration.

The cause of sudden death in RS is not fully understood, but alteration of brainstem cardiorespiratory center can be an attributing factor.

Neurochemical studies in the cerebrospinal fluid and brain tissues revealed the involvement of most systems of transmitters, their receptors, and trophic factors, including acetylcholine, dopamine, serotonin, glutamate, substance P, and the nerve growth factor. It is important to note their roles as neurotrophins in brain development and their later role in the normal function of mature brain.

Neuroimaging studies have revealed altered volume of specific areas of the cerebral cortex, such as the prefrontal, posterior frontal, and anterior temporal regions, and relative preservation of posterior temporal and posterior occipital regions.

A neuropathological report by Armstrong showed decreased brain weight to the level of a 1-year-old and decreased pigmentation of the substantia nigra pars compacta. The weight loss does not progress with age, indicating that it is not degeneration. No degenerative, demyelinating, or gross malformative process is recognized. The neuronal size is decreased and increased neuronal packing density is observed in the cortex and subcortical areas. Significant decrease of dendritic territories in the frontal, motor, and subcortical cortices was shown by Golgi technique. In the midbrain and substantia nigra, the large neurons of pars compacta have less melanin and tyrosine hydroxylase staining than controls. Limited studies of the brainstem suggest abnormalities in serotonin receptors and in the substance P content. These neuropathological findings suggest a failure of development. General autopsies show that all organs except the adrenal gland are small for age but not for height.

Studies using receptor autoradiography demonstrate abnormalities in the density of excitatory glutamate and inhibitory gamma-aminobutyric acid (GABA) synaptic receptors in postmortem brain tissue, supporting the hypothesis that RS is a genetic disorder of synapic development, especially that of the synapses that use glutamate and GABA as transmitters.

RS is a genetic disorder affecting mostly girls and is primarily a sporadic disorder with few familial cases.

Mutations in *MECP2*, X-linked gene encoding methyl-CpG-binding protein 2 (MeCP 2), in exons 1 to 4 or DNA deletions, represent the genetic cause of more than 90% of typical cases of RS.

The phenotype–genotype correlation has revealed that MECP2 correlates with clinical severity and characteristics. The *MECP2* mutation is also found in the case of some phenotypes of Angelman syndrome and autism.

The mutation can also be found in normal females or females with mild learning disability. The mutation type, pattern of X chromosome inactivation, or other unknown factors seem to play a role in these phenotypical variations.

The mutation is also found in males, and the phenotypes in males vary from fatal infantile encephalopathy to familial X-linked mental retardation. Classical RS can occur in males with somatic mosaicism or with Kleinfelter syndrome.

MECP2 mediates transcriptional silencing through its methyl-CpG-binding domain (MBD) and transcriptional repression domain (TRD), and modifies gene expression of its target genes. This epigenetic function seems to be significant in the genetic control in brain development.

In normal early embryonic life, MeCP2 is expressed in two developmentally important regions, that is, the medulla and the thalamus. In normal brain development, the neurons of the medulla express monoamines (noradrenaline and serotonin), which act as the critical trophic roles, and send nonspecific afferents to the developing cortex, where they influence migration and organization of neuronal systems. MeCP2 is also a marker of a maturing neuron, being increasingly expressed in neurons as they evolve. The increase in MeCp2 expression in the brain after the prenatal period suggests that MeCP2 might also be required for neuronal maintenance and function.

The abnormalities, observed in the features of clinical symptoms and signs as well as the chemical and anatomical findings, suggest that MeCP2 is essential for neuronal maturation of the specific systems. The signal for the initial expression of MECP2 in a neuronal precursor cell can be regulated by a cell-autonomous mechanism. Its increasing expression in fully matured neurons can then be regulated in part by external factors, such as

synaptic input. Thus, MECP2 appears to be required for both the structural and the functional maturity of the neurons.

The establishment of the *MECP2*-deficient mice displaying phenotypic features mimicking some symptoms of RS as well as the understanding of the function of *MECP2* at the cellular and molecular levels is developing.

Epidemiology/Risk Factors

Cases of RS have been reported worldwide among all ethnic backgrounds. The classical form of RS was reported to have a prevalence of about 1 in 10 000–15 000 girls.

The frequency may increase with the addition of atypical cases, variants, or formes fruste cases. Particularly, the discovery of the causative gene may increase the prevalence by clarifying the genetic bases of atypical, variants, or formes fruste cases. There are some geographical areas where the prevalence is higher.

There are no known risk factors for the occurrence of the disorder.

Clinical Features and Diagnostic Criteria

The clinical presentation of RS is characterized by the specific psychomotor developmental delay, and pathognomonic symptoms and signs, which appear in an age-dependent fashion.

The onset of the disorder was initially late infancy to early childhood after a seemingly normal development. However, placidity and mild muscle hypotonia are present from early infancy, and the onset of RS is believed to be in early infancy. Sleep–wake rhythm is abnormal with increased sleep during the day, starting from early infancy. These earliest clinical features are subtle in most of the cases and are often overlooked.

These clinical features are similar to the ones observed in autism, showing delayed development of the circadian sleep–wake rhythm and poor response to environmental stimulation.

In late infancy, failure to crawl, delayed development of voluntary hand use, and the deceleration of head growth are observed. From late infancy to early childhood, psychomotor regression and social withdrawal appear. This social withdrawal seen in this period and the aforementioned characteristics seen in early infancy comprise the autistic features of RS.

The most striking and pathognomonic symptom of RS is the stereotyped movements of the hands associated with the loss of purposeful hand use appearing at this period. The typical hand stereotypies are characterized by repetitive squeezing, flapping, clapping, wringing, or bizarre hand automatisms. These movements occur mostly in the midline and virtually continue during wakefulness.

Before these stereotypies manifest themselves, habit-like behaviors involving the hands are present, and excessive clapping may be present.

Stereotyped movement of the tongue and mouth and licking and teeth grinding are also characteristics.

These stereotypies are observed during wakefulness, and increase when the child gets excited or becomes anxious.

Age-dependent changes are also observed in the hand stereotypies, evolving from simple to complex and fast, then to slow and simple with age.

In early childhood, dystonic posture appears. Hand stereotypies are obscured by dystonic rigidity. Because of the dystonia, the stereotyped movements of the hands become fixed and this does not change through the rest of the course of the disease.

The pes varus or vulgus, dystonic posture of all extremities progresses after childhood. Kyphosis and scoliosis, which are the postural dystonia involving trunk, progress after childhood to adulthood in some patients.

The deceleration of the growth of the head begins in late infancy, and patients often become microcephalic after early childhood.

The characteristic gait was initially described as apraxic by Rett. However, both failure of crawling and gait dysfunction are due to failure of locomotion.

Epilepsy may be seen, but the severity is variable among individual cases.

Abnormal sleep–wake rhythm and inappropriate laughing or crying during wakefulness or sleep are also seen often.

Breathing abnormalities, such as hyperventilation, breath holding, air swallowing, and bloating are striking features seen in some RS. Heart rate variability, difficulty in swallowing, and constipation suggest autonomic impairment. Cold and small feet are also consistent with dysfunction of the autonomic nervous system.

Height, weight, and hand and foot sizes also decline later. Overweight or emaciation may be seen in some patients.

The age-dependent appearance of the clinical features has led to the proposal of staging the disease.

Because of the difficulty in understanding the complex clinical features, the efforts of constructing the diagnostic criteria were set in 1984 and in 1988. With the increase of reported cases and advances of the understanding of the pathophysiology of the disorder, some components of these diagnostic criteria need to be changed or deleted.

Differential Diagnosis

The diagnosis of RS is not difficult with careful history taking of characteristic symptoms and signs, and noting the age-dependent appearance of these symptoms and signs.

However, there are disorders that need to be differentiated from RS. They include for example autism and Angelman syndrome. Some female cases with autism, particularly the cases with regression during the course, may later prove to be RS. Infantile neuronal ceroid lipofuscinosis may show temporarily similar features to RS. Finally, some neurodevelopmental disorders may present with similar features with RS. Therefore, in these cases, some symptoms or some periods of the course may overlap with the features of RS.

X-linked-cyclin-dependent kinase-like 5 (CDKL5/STK9) has been proposed as another causative gene for RS, particularly early seizure cases with severe mental retardation.

Diagnostic Workup/Tests

The clinical features and their evolution at specific ages are typical of RS. Careful history taking and neurological examination leads to the correct diagnosis in most cases.

There are no pathognomonic laboratory, neurophysiological, or neuroradiological tests.

The finding of mutation of *MECP2* is the best test to clarify the diagnosis; however, it is important to keep in mind that there are cases even with typical clinical features that do not carry the *MECP2* mutation.

Management

Therapeutic approaches are still symptomatic, and unfortunately, no crucial treatments have been established. Rehabilitation, including physical and occupational therapy, and enhancement of communication with music therapy have been tried with limited results. Trials of theoretically attractive treatments in these areas have been reported. Medications directed to possible correction of the underlying pathomechanisms have failed to produce appreciative and sustained effects.

Seizure is one of the common symptoms of RS that appears in early childhood. In such cases, administration of a suitable anticonvulsant(s) is essential. However, there is no antiepileptics specifically recommended for RS, and some cases can be drug resistant.

The effort to control the abnormal respiratory patterns is another challenge. Each abnormal respiratory pattern requires unique and special intervention. Some of the phenotypes can partly respond to pharmacological intervention, but others do not.

When physical therapy and orthopedic management of scoliosis fail, surgical treatments are indicated.

With some patients, management of nutrition becomes necessary, including gastrostomy.

General health care and prompt appropriate management for the undercurrent or acute illnesses is also important. All necessary managements for better quality of life need to be considered.

Prognosis

Initially, RS was thought to be progressive, but the clinical course is basically one of a developmental disorder.

As for the life-expectancy, relatively healthy patients survive into the fourth and fifth decades, although there is an increased incidence of sudden death in adolescent years. Cases surviving into their seventieth have been reported.

Further Reading

Amir RE, Van den Veyver IB, Wan M, et al. (1999) Rett syndrome is caused by mutations in X-linked MECP2, encoding methyl-CpG-binding protein 2. *Nature Genetics* 23(2): 127–128.

Armstrong DD (1997) Review of Rett syndrome. *Journal of Neuropathology and Experimental Neurology* 56(8): 843–849.

Chen RZ, Akbarian S, Tudor M, and Jaenisch R (2001) Deficiency of methyl-CpG binding protein-2 in CNS neurons results in a Rett-like phenotype in mice. *Nature Genetic* 27(3): 327–331.

Guy J, Hendrich B, Holmes M, Martin JE, and Bird A (2001) A mouse Mecp2-null mutation causes neurological symptoms that mimic Rett syndrome. *Nature Genetics* 27(3): 322–326.

Hagberg B (ed.) (1993) *Rett Syndrome-Clinical & Biological Aspects.* London: Mac Keith Press.

Hagberg B and Witt-Engerström I (1986) Rett syndrome: A suggested staging system for describing impairment profile with increasing age towards adolescence. *American Journal of Medical Genetics. Supplement* 1: 47–59.

Hagberg B, Goutières F, Hanefeld F, et al. (1985) Rett syndrome: criteria for inclusion and exclusion. *Brain and Development* 7(3): 372–373.

Hagberg B, Aicardi J, Dias K, and Ramos O (1983) A progressive syndrome of autism, dementia, ataxia, and loss of purposeful hand use in girls: Rett's syndrome: Report of 35 cases. *Annals of Neurology* 14(4): 471–479.

Ishikawa A, Goto T, Narasaki M, et al. (1985) A new autistic tendency: A report of three cases. *Brain and Development* 3: 258.

(2005) *Journal of Child Neurology* 9.

Kerr A and Witt-Engerström I (eds.) (2001) *Rett Disorder and the Developing Brain.* New York: Oxford University Press.

Leiber B and Olbrich G (1972) *Die klinischen Syndrome bei Hyperammonämie*, p. 763. Munich: Urban & Schwarzenberg.

Nomura Y, Segawa M, and Hasegawa M (1984) Rett syndrome – Clinical studies and pathophysiological consideration. *Brain and Development* 6(5): 475–486.

Rett A (1966) *Über ein Cerebral-Atrophisches Syndrombei Hyperammonämie.* Wien: Brüder Hollinek.

Rett A (1977) Cerebral atrophy associated with hyperammonaemia. In: Vinken PJ and Bruyn GW (eds.) *Handbook of Clinical Neurology*, vol 29, pp. 305–329. Amsterdam: North-Holland.

The Rett Syndrome Diagnostic Criteria Work Group (1988) Diagnostic criteria for rett syndrome. *Annals of Neurology* 23: 425–428.

RADIATION RESEARCH 175, 83–89 (2011)
0033-7587/11 $15.00

DOI: 10.1667/RR2092.1

Differential Role of DNA-PKcs Phosphorylations and Kinase Activity in Radiosensitivity and Chromosomal Instability

Hatsumi Nagasawa,[a] John B. Little,[b] Yu-Fen Lin,[c] Sairei So,[c] Akihiro Kurimasa,[d] Yuanlin Peng,[a] John R. Brogan,[a] David J. Chen,[c] Joel S. Bedford[a] and Benjamin P. C. Chen[a,1]

[a] *Department of Environmental and Radiological Health Sciences, Colorado State University, Fort Collins, Colorado 80523;* [b] *Center for Radiation Sciences and Environmental Health, Harvard School of Public Health, Boston, Massachusetts 02115;* [c] *Department of Radiation Oncology, University of Texas Southwestern Medical Center at Dallas, Dallas, Texas, 75390; and* [d] *Institute of Regenerative Medicine and Biofunction, Graduate School of Medical Science, Tottori University, Tottori, Japan, 683-8503*

Nagasawa, H., Little, J. B., Lin, Y-F., So, S., Kurimasa, A., Peng, Y., Brogan, J. R., Chen, D. J., Bedford, J. S. and Chen, B. P. C. Differential Role of DNA-PKcs Phosphorylations and Kinase Activity in Radiosensitivity and Chromosomal Instability. *Radiat. Res.* 175, 83–89 (2011).

The catalytic subunit of DNA-dependent protein kinase (DNA-PKcs) is the key functional element in the DNA-PK complex that drives nonhomologous end joining (NHEJ), the predominant DNA double-strand break (DSB) repair mechanism operating to rejoin such breaks in mammalian cells after exposure to ionizing radiation. It has been reported that DNA-PKcs phosphorylation and kinase activity are critical determinants of radiosensitivity, based on responses reported after irradiation of asynchronously dividing populations of various mutant cell lines. In the present study, the relative radiosensitivity to cell killing as well as chromosomal instability of 13 DNA-PKcs site-directed mutant cell lines (defective at phosphorylation sites or kinase activity) were examined after exposure of synchronized G_1 cells to ^{137}Cs γ rays. DNA-PKcs mutant cells defective in phosphorylation at multiple sites within the T2609 cluster or within the PI3K domain displayed extreme radiosensitivity. Cells defective at the S2056 cluster or T2609 single site alone were only mildly radiosensitive, but cells defective at even one site in both the S2056 and T2609 clusters were maximally radiosensitive. Thus a synergism between the capacity for phosphorylation at the S2056 and T2609 clusters was found to be critical for induction of radiosensitivity.

INTRODUCTION

DNA double-strand breaks (DSBs) are the principal lesions responsible for the major biological effects of radiation. Such DSBs can be repaired in mammalian cells by at least two major pathways: nonhomologous end joining (NHEJ), which operates throughout the cell cycle, or homologous recombination repair (HRR), which operates during S or G_2 (*1*). The NHEJ pathway uses several enzymes that capture both DNA ends and bring them together in a synaptic complex to facilitate direct ligation of the DNA break (*2*). One of the first enzymes to be attracted to DSBs is the Ku70/80 heterodimer; subsequently, the DNA-Ku70/80 scaffold recruits a large 460-kDa serine/threonine kinase called the DNA-dependent protein kinase catalytic subunit (DNA-PKcs). The protein complex formed after the association of both Ku70/80 and DNA-PKcs at the DNA ends is generally referred to as the DNA-dependent protein kinase (DNA-PK). DNA-PK kinase activity was shown to be dependent on the functional Ku protein (*3, 4*). The xrs-6 cells defective in Ku DNA binding lack DNA-PK activity and DSB repair, both of which can be restored in xrs-6 cells by introducing wild-type Ku80 (*3*).

A greater degree of radiosensitivity has been reported in terms of the extent of DNA repair, cell killing and chromosomal aberrations in Ku-deficient cells than in DNA-PKcs-deficient cells (*5–7*). In addition, Ku70/80-deficient xrs-5 and -6 cells have been reported to have greatly reduced cellular repair throughout cell cycle, no radiation dose-rate effect, and no repair of potentially lethal damage (*8*). The cell cycle effect in particular appears to be significantly different in Ku70/80-deficient cells and DNA-PKcs-deficient cells (*9–14*).

Several activities of DNA-PKcs have been shown to contribute its function in DSB repair, including the intrinsic kinase activity and phosphorylation. The kinase activity of DNA-PKcs is essential for DSB repair (*15*), likely through phosphorylation and regulation of NHEJ factors including DNA-PKcs itself (*2*). Thus far, many phosphorylation residues of DNA-PKcs have been identified both *in vitro* and *in vivo* (*16–22*). Most of the DNA-PKcs phosphorylation sites are in the S/TQ motifs (serine or threonine followed by a glutamine residue)

[1] Address for correspondence: Department of Radiation Oncology, University of Texas Southwestern Medical Center at Dallas, 2201 Inwood Rd., Rm. NC7.502, Dallas, TX 75390-9187; e-mail: benjamin.chen@utsouthwestern.edu.

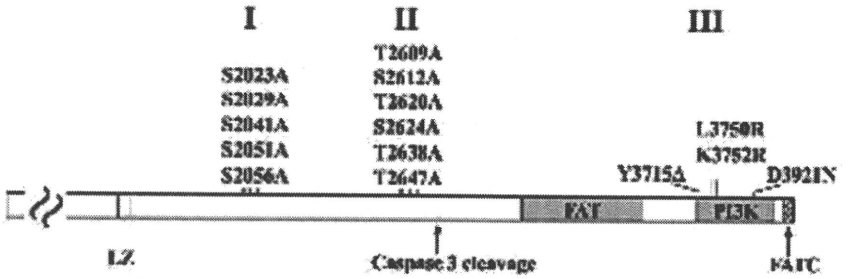

FIG. 1. Summary of DNA-PKcs mutations within the S2056 cluster, T2609 cluster and PI3K kinase domain. I, S2056 phosphorylation cluster (refs. *16 18*). II, T2609 phosphorylation cluster (refs. *19, 20*). III, PI3K domain (ref. *15*).

commonly present in many DNA damage repair proteins and are the cognate substrates of PIKK kinases (*23*). In addition, the critical phosphorylation residues of DNA-PKcs are largely concentrated at the T2609 and the S2056 clusters (*16 20*). Although the mechanism for DNA-PKcs phosphorylation remains to be clarified, as is the case for its kinase activity, DNA-PKcs phosphorylation is required for DSB repair.

The present study was designed to measure and compare the relative radiosensitivity of G_0/G_1 synchronized site-directed mutant cells involving phosphorylatable residues of the T2609 cluster (*16 18*), the S2056 cluster (*19, 20*), and the carboxyl-terminus PI3K domain (*15*) of DNA-PKcs. Radiosensitivity examined in asynchronous randomly dividing cell populations may be dependent on the cell line because it represents the average response of a mixture of cells in different phases of the cell cycle, particularly of cells in the most radioresistant phases (*24–26*). In such instances the contributions of other processes such as HRR greatly complicate the interpretation of results. We have thus chosen to study synchronized cell populations in which repair will occur primarily via the NHEJ pathway to reduce the confounding factor of differences in cell cycle distribution among different cell lines.

MATERIALS AND METHODS

Cell Lines and Cell Culture

For these studies, we employed the wild-type Chinese hamster cell lines CHO (*27*) and AA8 (*28*), NHEJ-deficient xrs-5 cells (*29*) and V3 cells (*10*), and cell lines derived from DNA-PKcs null V3 cells with complemented human DNA-PKcs cDNA containing amino acid substitutions at various positions that are described in Fig. 1 and Table 1 (*15, 16, 18, 19*). The cells were maintained at 37°C in a humidified 95% air/5% CO_2 atmosphere in Eagle's minimal essential medium (MEM, containing 52 mg/liter isoleucine) supplemented with 10% heat-inactivated fetal bovine serum, penicillin (50 μg/ml), and streptomycin (50 mg/ml). When the cultures approached 30% confluence in T-25 tissue culture flasks, the normal growth medium was removed. The medium was then changed twice at 24-h intervals to isoleucine-deficient MEM containing 5% 3× dialyzed fetal bovine serum to synchronize the cells in G_0/G_1 phase. The experiments were initiated 1 day after the second medium change. At this time the cells were synchronized in G_0/G_1 phase (*30*). Cells were pulse labeled with 30 μ*M* BrdU for 15 min and then fixed in 70% ethanol. Fixed cells were treated with 0.1 mg/ml RNase A and 3N HCl sequentially for 30 min at 37°C, then incubated with BrdU antibody conjugated with Alexa Fluor 488 (Invitrogen) for 2 h at 37°C. The cells were analyzed using a FACScan flow cytometer and CellQuest software (BD Biosciences). Although more than 10% S-phase cells were observed in some of the cell lines, others showed many fewer S-phase cells after IL-deficient synchronization as shown in Table 2. The mean doubling time was determined from the linear portion of the growth curves of the exponentially growing cell population.

Irradiation and Colony Formation

Synchronized G_0/G_1 cells were irradiated aerobically at room temperature. The radiation source was a J. L. Shepherd and Associates irradiator that emitted ^{137}Cs γ rays at a dose rate of 2.5 Gy/min. Survival curves were obtained by measuring the colony-forming ability of irradiated cell populations. Cells were plated postirradiation onto 100-mm plastic petri dishes and incubated for 7–10 days for colony formation. The dishes were then fixed with 100% ethanol and stained with 0.1% crystal violet solution. A colony with more than 50 cells was scored as a survivor.

Chromosome Analysis

Exponentially growing cells were irradiated with ^{137}Cs γ rays at a dose rate of 2.5 Gy/min. Colcemid was added to a final concentration of 1 μg/ml starting at 30 min after irradiation, and the cells were harvested 4 h later so that the mitotic cells collected would have been in late-S/G_2 phase at the time of irradiation (*48*). Mitotic cells were harvested by trypsinization and hypotonic treatment. Cells were fixed in methanol:acetic acid (3:1) and chromosomes were spread by air-drying (*31*). After the slides were stained with Giemsa, chromosome aberrations were scored.

RESULTS AND DISCUSSION

In a study using asynchronous exponentially growing cells, it was reported that DNA-PKcs cell lines containing site-directed mutation at the S2056/T2609 clusters as well as the C-terminal phosphatidylinositol 3-kinase (PI3K) kinase domain were radiosensitive (*15 20*). The synchronized DNA-PKcs mutant cell lines irs-20 and V3 were very radiosensitive when irradiated in the G_1 phase (nearly the same as Ku80-deficient xrs-5 cells) but displayed rapidly increasing cell survival (decreasing radiosensitivity) when they were irradiated throughout S phase, peaking at late S phase and then declining (*13, 19, 32*). Because other DNA repair

TABLE 1
Cell Lines Derived from DNA-PKcs Null V3 Cells with Complemented Human DNA-PKcs cDNA Containing Amino Acid Substitutions at Various Positions in the DNA-PKcs Constructs

Coded mutant cell lines	Altered DNA-PKcs mutants (complemented cDNA)	Substituted domains													
		S2056 cluster[a]					T2609 cluster[a]						PI3K[b,c,d,e]			
		S2023	S2029	S2041	S2051	S2056	T2609	S2612	T2620	S2624	T2638	T2647	Y3715	L3750	K3752	D3921
L-1	Wild-type															
L-2	V3-7A (S2056A + T2609 cluster to A)					A	A	A	A	A	A	A				
L-3	V3-6A (T2609 cluster to A)						A	A	A	A	A	A				
L-4	V3-2A (S2056A/T2609A)					A	A									
L-5	V3-S2056A					A										
L-6	V3-T2609A						A									
L-7	V3 (empty vector)															
L-8	V3-KA4 (kinase dead)														R	
L-9	V3-KB20 (kinase dead)													R	R	
L-10	V3-KC23 (kinase dead)												Δ			
L-11	V3-KD51 (kinase dead)															N
L-12	V3-5A (S2056 cluster to A)	A	A	A	A	A										
L-14	V3-3A (T2609A/T2638A/T2647A)						A				A	A				

[a] Serine (S) and threonine (T) substituted by alanine (A) in the S2056 and T2609 cluster sites.
[b] V3-KC23 mutant carries a frame-shift at position of amino acid 3715 that resulted in truncation of the protein after 10 amino acids and loss of the entire PI3K kinase domain.
[c] V3-KA4 mutant substituted lysine 3752 (K3752) to arginine (R).
[d] V3-KB20 mutant substituted leucine 3750 (L3750) and K3752 to arginine (R).
[e] V3-KD51 mutant substituted aspartic acid (D) to asparagine (N).

processes such as IIRR also contribute to survival but operate virtually exclusively during S and G_2, it is important to study radiosensitivity with synchronous G_1-phase cells for proper interpretation of results. The present study was performed with cells incubated in isoleucine-deficient medium to synchronize the cell populations in G_2/G_1 phase (*30*). The radiosensitivity of cells synchronized in G_1 by isoleucine deprivation is

TABLE 2
Characteristics of Nonirradiated Chinese Hamster Cell Lines

Cell line	Type of mutation	Percentage of S-phase cells[a]		MDT (h)[b]	Model chromosome no. per cell (%)[c]
		IL[-]	Asyn		
CHO	Wild-type	3.4	61.5	14	21 (39.3)
AA8	Wild-type	1.4	54.5	13	20 (40.0)
Xrs5	Ku80 null	10.5	51.0	18	20 (32.0)
L-1	Wild-type	2.1	47.0	16	21 (19.0)
L-2	DNA-PKcs	5.6	43.4	15	34 (32.0)
L-3	DNA-PKcs	7.7	43.3	14	30 (33.0)
L-4	DNA-PKcs	5.2	51.2	15	35 (21.0)
L-5	DNA-PKcs	2.3	45.8	16	20 (19.6)
L-6	DNA-PKcs	12.2	49.8	17	20 (50.0)
L-7	DNA-PKcs null	0.8	59.8	18	20 (25.0)
L-8	DNA-PKcs	13.4	48.6	18	20 (41.0)
L-9	DNA-PKcs	13.1	52.2	14	33 (24.0)
L-10	DNA-PKcs	12.1	51.0	18	21 (52.0)
L-11	DNA-PKcs	2.4	50.6	16	20 (44.0)
L-12-10[d]	DNA-PKcs	6.7	50.5	26	30 (18.0)
L-12-15[d]	DNA-PKcs	2.0	48.2	16	33 (17.0)
L-14	DNA-PKcs	6.1	42.7	25	36 (18.0)

[a] Percentage of cells incorporating IdrdU during a 15-min pulse-labeling after 48 h IL-deficient synchronization or in asynchronous cell population.
[b] Mean doubling time (MDT) was determined from the linear portion of growth curves of the exponentially growing cell population.
[c] Model chromosome number per cell. More than 100 metaphase cells were scored for each cell line. No significant differences in ploidy were found between nonirradiated and irradiated cells. Numbers in parentheses are percentages of cells scored with model chromosome number.
[d] Two clones were isolated separately as independent mutant clones.

TABLE 3
Gamma-Ray Sensitivity and Chromosomal Aberration Induced in DNA-PK Mutant Cell Lines

Cell line	Type of mutation	D_0 (Gy)[a]	D_{10} (Gy)[b]	Total chromosome aberrations per cell[c]		Radiation sensitivity[d]
				0 (Gy)	0.5 (Gy)	
CHO	Wild-type	1.17 ± 0.03	4.13 ± 0.19	0.019 (159)	0.057 (159)	N
AA8	Wild-type	1.35 ± 0.10	4.55 ± 0.19	0.038 (159)	0.094 (159)	N
Xrs5	Ku80 null	0.68 ± 0.04	0.72 ± 0.02	0.110 (106)	1.450 (106)	SSS
L-1	Wild-type	1.08 ± 0.05	3.50 ± 0.46	0.019 (53)	0.170 (53)	N
L-2	DNA-PKcs	0.37 ± 0.02	1.14 ± 0.05	0.153 (53)	0.271 (53)	SSS
L-3	DNA-PKcs	042 ± 0.03	1.12 ± 0.08	0.135 (159)	0.574 (53)	SSS
L-4	DNA-PKcs	0.47 ± 0.04	1.20 ± 0.07	0.128 (53)	0.275 (53)	SSS
L-5	DNA-PKcs	0.96 ± 0.06	2.87 ± 0.15	0.075 (53)	0.094 (53)	S
L-6	DNA-PKcs	0.92 ± 0.08	2.64 ± 0.14	0.075 (53)	0.171 (53)	S
L-7	DNA-PKcs null	0.36 ± 0.02	1.09 ± 0.04	0.094 (53)	0.660 (53)	SSS
L-8	DNA-PKcs	0.38 ± 0.03	1.00 ± 0.05	0.059 (53)	0.563 (30)	SSS
L-9	DNA-PKcs	0.39 ± 0.04	1.14 ± 0.20	0.039 (53)	0.270 (53)	SSS
L-10	DNA-PKcs	0.46 ± 0.02	1.21 ± 0.06	0.057 (106)	0.547 (106)	SSS
L-11	DNA-PKcs	0.36 ± 0.02	1.15 ± 0.05	0.094 (53)	0.226 (53)	SSS
L-12-10	DNA-PKcs	0.75 ± 0.06	2.25 ± 0.39	0.189 (53)	0.389 (53)	SS
L-12-15	DNA-PKcs	0.70 + 0.12	2.11 + 0.09	0.094 (106)	0.554 (106)	SS
L-14	DNA-PKcs	0.63 ± 0.02	1.50 ± 0.10	0.100 (53)	0.179 (53)	SS

[a] D_0, a parameter in the multitarget equation ($S = 1 - [1 - \exp(-D/D_0)]^n$): the radiation dose that reduces survival to e^{-1} (i.e. 0.375) of its previous value on the exponential portion of the survival curve. Each point represents of the mean ± SEM of the results from more than three separate experiments.

[b] D_{10}, radiation dose required to reduce survival to 10%.

[c] Frequencies of chromosomal aberrations were normalized to 21 chromosome per cell based on modal chromosome number per cell (Table 2). Numbers in parentheses are numbers of cells scored.

[d] Radiosensitivity based on the D_0 value: N, normal (D_0 1.0–1.4 Gy); S, slightly sensitive (D_0 0.9 Gy); SS, sensitive (D_0 0.6–0.9 Gy); SSS, very sensitive (D_0 0.35–0.7 Gy).

similar to that of cells synchronized in G_1 by allowing harvested mitotic cells to progress into G_1 (*33*).

The experiments were carried out after all cell line designations were coded blindly as lines 1–12 and 14 without knowing the genotype of each cell line. Radiation effects on survival and chromosomal aberrations were examined in the site-directed mutant cell lines with mutations at the S2056 cluster, the T2609 cluster and the PI3K domain (Table 1 and Fig. 1). Table 3 shows cell killing after irradiation in G_0/G_1 as well as radiation-induced total chromosomal aberrations in late S/G_2-phase cells among the various Chinese hamster cell lines compared to the DNA-PKcs site-directed mutant cell lines. We measured the D_0 and D_{10} from complete survival curves for determining relative radiosensitivity as described in the last column and footnotes in Table 3. These survival curves are shown graphically in Fig. 2.

Both the L-2 and L-3 cell lines contain the mutated T2609 cluster, in which all six serine/threonine sites were replaced with alanine (A). When irradiated in the G_0/G_1 phase, these cell lines were very radiosensitive and fell in the same shaded area on the dose–survival plot as xrs-5 and V3 cells (L-7 empty vector) (Fig. 2A). L-14 cells also containing a mutated T2609 cluster with three threonine residues were replaced with alanine (T2609A/T2638A/T2674A) and showed intermediate radiosensitivity, but they were more radiosensitive than L-6 cells, in which only a single amino acid was replaced (T2609A) (Fig. 2A).

The single-site replacement of alanine in L-5 (S2056A) and L-6 (T2609A) mutant cell lines resulted in only mild hypersensitivity to radiation. However, L-4 (S2056A/T2609A) cells displayed synergistically increased radiosensitivity compared to cell lines with complete loss of the T2609 cluster (L-3) or complete loss of the S2056 cluster. The hyper-radiosensitivity of L-4 cells in G_0/G_1 is distinctive from the mild radiosensitivity when exponentially growing cells were irradiated, whereas L-5 (S2056A) cells showed similar radiosensitivity to γ rays in G_0/G_1 phase or in asynchronous conditions (*18, 19*).

It has been reported that the measurement of NHEJ direct end joining relative to alternative microhomology-directed end-joining activity increased dramatically in cells defective in NHEJ compared to the normal cell lines (*34*). Although there was no significant difference in ionizing radiation-induced cell killing between S2056A (L-5) and S2056A/T2609A (L-4) cells when they were irradiated in asynchronous cultures, measurement of microhomology-directed end joining showed a significant increase (~80%) in S2056A/T2609A (L-4) cells as well as in V3 (L-7) cells, whereas S2056A (L-5) and T2609A (L-6) cells showed less induction (~60%) of microhomology-directed end joining (*19*). The difference in microhomology-directed end joining suggests that NHEJ repair is severely compromised in L-4 (S2056A/T2609A) cells, reflecting the hyper-radiosensitivity of L-4 cells irradiated in G_0/G_1. The results also implied that

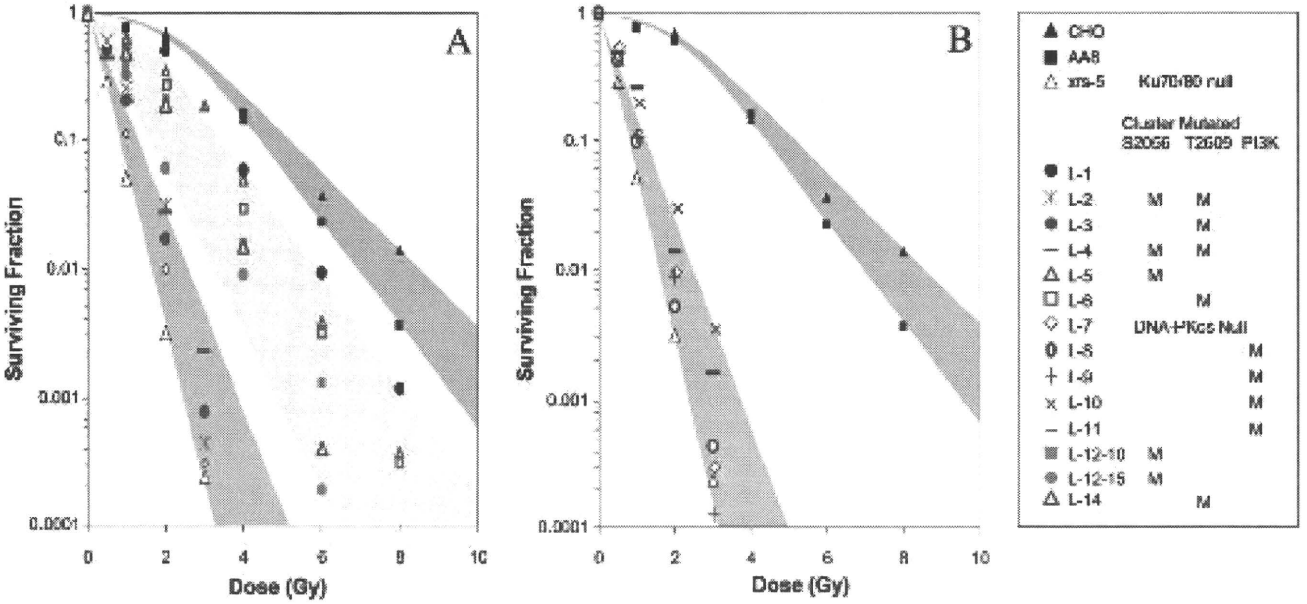

FIG. 2. Panel A: Survival curves of site-directed mutant cell lines with amino acid replacement in the S2056 and T2609 clusters. Colored areas indicate differential radiosensitivities: green, D_0 – 1.0–1.4 Gy; yellow, D_0 – 0.6–0.9 Gy; red, D_0 – 0.35–0.7 Gy. Panel B: Survival curves of site-directed mutant cell lines with replacement of amino acid or frame-shift mutation on PI3K domain. Colored areas indicate differential radiosensitivities as described above.

the two sites (S2056 and T2609) may have some kind of interaction or synergistic effect on radiosensitivity. It is not clear why there are large differences in sensitivity for radiation-induced cell killing between L-4 and L-5/L-6 cells. Although the S2056 and T2609 clusters are 553 amino acids apart (Fig. 1), this does not exclude a closer location that depends on the three-dimensional structure of DNA-PKcs leading to synergistic interaction that could increase radiosensitivity in the L-4 cell line.

The kinase activity of DNA-PKcs is essential for NHEJ repair because kinase-dead DNA-PKcs mutant cell lines (L-8, -9, -10 and -11) with site-directed mutations within the conserved PI3K domain significantly lowered DNA-PKcs kinase activity and increased radiosensitivity, even though they contained different amino acid substitutions or truncation (*15*). All four kinase-dead mutant cell lines were very sensitive when the cells were irradiated in G_2/G_1 phase (Table 3 and Fig. 2B) and displayed five to ten times greater radiosensitivity in G_2/G_1 phase than in asynchronous cell populations with 2 Gy (*15*).

In addition to investigating radiosensitivity of each mutant cell lines in G_0/G_1, we found that aneuploidy occurred in several DNA-PKcs mutant cell lines, as shown in Table 2. The L-2 and L-3 cell lines, in which all six phosphorylation residues of the T2609 cluster were substituted to alanine, were both very radiosensitive and aneuploid. Aneuploidy was also found in L-4 (S2056A/T2609A) cells but not in the single-site mutated L-5 (S2056A) and L-6 (T2609A) cell lines. On the other hand, two L-12 cell lines (L-12-10, L-12-15) in which all five putative phosphorylation residues of the S2056 cluster were substituted to alanine showed only mild radiosensitivity in G_0/G_1 phase (Table 3 and Fig. 2A) but displayed severe aneuploidy (Table 2). All four kinase-dead mutant cell lines with different types of mutations at the PI3K domain were very radiosensitive (Table 3 and Fig. 2B), but only the L-9 cell line was aneuploid (Table 2). While there was no direct cause-and-effect relationship seen between aneuploidy and radiosensitivity, it cannot be ruled out that certain DNA-PKcs mutations can lead to a propensity to develop aneuploidy.

Total spontaneous chromosomal aberrations as well as chromosomal aberrations induced by 0.5 Gy γ rays in G_2 were analyzed in wild-type (CHO and AA8) and NHEJ mutated cells (Ku 70/80 deficient xrs-5 and DNA-PKcs site-directed mutant cell lines). There were higher frequencies of spontaneous chromosomal aberrations in NHEJ mutated cells than in wild-type CHO and AA8 cells (Table 3). This may suggest that these mutant cell lines developed genetic instability and/or aneuploidy during the process of establishing stable mutant clones (Tables 2 and 3). An assay of radiation-induced G_2 chromosomal aberrations was performed by irradiating exponentially growing cells followed by 4 h of Colcemid treatment starting 30 min after irradiation. Mitotic cells collected under this protocol would have been in late S/G_2 phase at the time of irradiation (*48*). The G_2-phase chromosomal assay has been applied to number of radiosensitivity and cancer predisposition syndromes (*35–38*). Chinese hamster cells deficient in either NHEJ or HRR showed similar increases in radiation-induced chromosomal aberrations in late S/G_2 phase (*39–42*).

After 0.5 Gy of γ rays, total chromosomal aberrations in late S/G_2-phase cells were also significantly elevated for all NHEJ mutant cell lines compared with the wild-type CHO and AA8, except the L-5 and L-6 cell lines (Table 3). These two cell lines showed near normal radiosensitivities and near diploid chromosome numbers (Tables 2 and 3). It is notable that L-12 cells, which contain the mutated S2056 cluster, in which all five serine sites were replaced with alanine, displayed a high frequency of spontaneous and radiation-induced chromosomal aberrations, although L-12 cells showed only mild radiosensitivity in G_0/G_1 phase (Table 3 and Fig. 2A).

The relationship between DNA-PKcs activity and DSB repair underlying the NHEJ mechanism has been widely studied. Results from the current study provide further insight into the contributions of different modifications of DNA-PKcs activity (phosphorylations and kinase activity) to radiosensitivity phenotypes in G_0/G_1-phase cells. Mice deficient in DNA-PKcs and NHEJ components have been characterized by increased sensitivity to agents causing DNA damage as well as to chromosomal instability, immunodeficiency and predisposition to thymic lymphomas (*43*). Studies of clinical samples have also correlated DNA-PKcs activity with cancer risk and prognosis. A reduction of DNA-PKcs expression or DNA-PK kinase activity in peripheral blood lymphocytes (PBL) has been found in bronchial epithelial cells (a progenitor cell for lung cancer) (*44*) and was associated with a risk for breast and uterine cervix cancer as well as an increased frequency of chromosomal aberrations (*45*). Negative expression of DNA-PKcs has also been correlated with tumor progression and poor patient survival in gastric cancer (*46*). Recently, several point mutations of DNA-PKcs have been identified in breast tumor samples; one such mutation, Thr2609Pro, occurred specifically at the T2609 phosphorylation cluster (*47*). Taken together, these results suggest a tumor suppressor role of DNA-PKcs in the development of cancer.

In summary, this study focused on radiosensitivity and chromosomal instability in site-directed DNA-PKcs mutant cell lines after γ irradiation in the G_0/G_1 phase. Very clear differences in radiosensitivity were observed among cell lines mutated in the T2609 cluster, the S2056 cluster and the PI3K kinase domain. Additionally, an interesting synergism between defects in phosphorylation sites that occur together in both the S2056 and T2609 clusters was found to be critical for conferring maximum hypersensitivity to radiation-induced cell killing, comparable to DNA-PKcs null mutants.

ACKNOWLEDGMENTS

This research was supported by grants DE-FG02-07ER64350 (HN, JSB) and DEFG02-05ER65089 (JBL) from the U.S. Department of Energy Office of Biological and Environmental Research Low Dose Radiation Research Program, NNX07AP84G (BPC) from National Aeronautics and Space Administration Space Radiation Research Program, and NCI/NIH grant CA50519 (DJC) from the U.S. Department of Health and Human Services. Appreciation is expressed Jennifer A. Hufnagle and Trenton Wade for technical assistance in these experiments.

Received: November 21, 2009; accepted: April 7, 2010; published online: November 17, 2010

REFERENCES

1. L. H. Thompson and C. L. Limoli, Origin, recognition, signaling and repair of DNA double-strand breaks in mammalian cells. In *Eukaryotic DNA Damage Surveillance and Repair* (K. Caldecott Ed.), pp. 107–145. Springer, Berlin, Heidelberg, New York, 2004.
2. E. Weterings and D. J. Chen, The endless tale of non-homologous end-joining. *Cell Res.* **18**, 114–124 (2008).
3. N. J. Finnie, T. M. Gottlieb, T. Blunt, P. A. Jeggo and S. P. Jackson, DNA-dependent protein kinase activity is absent in xrs-6 cells: implications for site-specific recombination and DNA double-strand break repair. *Proc. Natl. Acad. Sci. USA* **92**, 320–324 (1995).
4. S. R. Peterson, A. Kurimasa, M. Oshimura, W. S. Dynan, E. M. Bradbury and D. J. Chen, Loss of the catalytic subunit of the DNA-dependent protein kinase in DNA double-strand-break-repair mutant mammalian cells. *Proc. Natl. Acad. Sci. USA* **92**, 3171–3174 (1995).
5. J. B. Little, H. Nagasawa, G. C. Li and D. J. Chen, Involvement of the nonhomologous end joining DNA repair pathway in the bystander effect for chromosomal aberrations. *Radiat. Res.* **159**, 262–267 (2003).
6. H. Nagasawa and J. B. Little, Bystander effect for chromosomal aberrations induced in wild-type and repair deficient CHO cells by low fluences of alpha particles. *Mutat. Res.* **508**, 121–129 (2002).
7. H. Nagasawa, J. B. Little, W. C. Inkret, S. Carpenter, M. R. Raju, D. J. Chen and G. F. Strniste, Response of X-ray-sensitive CHO mutant cells (xrs-6c) to radiation. II. Relationship between cell survival and the induction of chromosomal damage with low doses of alpha particles. *Radiat. Res.* **126**, 280–288 (1991).
8. H. Nagasawa, D. J. Chen and G. F. Strniste, Response of X-ray-sensitive CHO mutant cells to gamma radiation. I. Effects of low dose rates and the process of repair of potentially lethal damage in G_1 phase. *Radiat. Res.* **118**, 559–567 (1989).
9. G. E. Iliakis and R. Okayasu, Radiosensitivity throughout the cell cycle and repair of potentially lethal damage and DNA double-strand breaks in an X-ray-sensitive CHO mutant. *Int. J. Radiat. Biol.* **57**, 1195–1211 (1990).
10. G. F. Whitmore, A. J. Varghese and S. Gulyas, Cell cycle responses of two X-ray sensitive mutants defective in DNA repair. *Int. J. Radiat. Biol.* **56**, 657–665 (1989).
11. J. Y. Lin, M. C. Muhlmann-Diaz, M. A. Stackhouse, J. F. Robinson, G. E. Taccioli, D. J. Chen and J. S. Bedford, An ionizing radiation-sensitive CHO mutant cell line: irs-20. IV. Genetic complementation, V(D)J recombination and the scid phenotype. *Radiat. Res.* **147**, 166–171 (1997).
12. A. Priestley, H. J. Beamish, D. Gell, A. G. Amatucci, M. C. Muhlmann-Diaz, B. K. Singleton, G. C. Smith, T. Blunt, L. C. Schalkwyk and G. E. Taccioli, Molecular and biochemical characterisation of DNA-dependent protein kinase-defective rodent mutant irs-20. *Nucleic Acids Res.* **26**, 1965–1973 (1998).
13. M. A. Stackhouse and J. S. Bedford, An ionizing radiation-sensitive mutant of CHO cells: irs-20. II. Dose-rate effects and cellular recovery processes. *Radiat. Res.* **136**, 250–254 (1993).
14. M. A. Stackhouse and J. S. Bedford, An ionizing radiation-sensitive mutant of CHO cells: irs-20. III. Chromosome

aberrations, DNA breaks and mitotic delay. *Int. J. Radiat. Biol.* **65**, 571–582 (1994).

15. A. Kurimasa, S. Kumano, N. V. Boubnov, M. D. Story, C. S. Tung, S. R. Peterson and D. J. Chen, Requirement for the kinase activity of human DNA-dependent protein kinase catalytic subunit in DNA strand break rejoining. *Mol. Cell. Biol.* **19**, 3877–3884 (1999).

16. D. W. Chan, B. P. Chen, S. Prithivirajsingh, A. Kurimasa, M. D. Story, J. Qin and D. J. Chen, Autophosphorylation of the DNA-dependent protein kinase catalytic subunit is required for rejoining of DNA double-strand breaks. *Genes Dev.* **16**, 2333–2338 (2002).

17. Q. Ding, Y. V. Reddy, W. Wang, T. Woods, P. Douglas, D. A. Ramsden, S. P. Lees-Miller and K. Meek, Autophosphorylation of the catalytic subunit of the DNA-dependent protein kinase is required for efficient end processing during DNA double-strand break repair. *Mol. Cell. Biol.* **23**, 5836–5848 (2003).

18. B. P. Chen, N. Uematsu, J. Kobayashi, Y. Lerenthal, A. Krempler, H. Yajima, M. Lobrich, Y. Shiloh and D. J. Chen, Ataxia telangiectasia mutated (ATM) is essential for DNA-PKcs phosphorylations at the Thr-2609 cluster upon DNA double strand break. *J. Biol. Chem.* **282**, 6582–6587 (2007).

19. B. P. Chen, D. W. Chan, J. Kobayashi, S. Burma, A. Asaithamby, K. Morotomi-Yano, E. Botvinick, J. Qin and D. J. Chen, Cell cycle dependence of DNA-dependent protein kinase phosphorylation in response to DNA double strand breaks. *J. Biol. Chem.* **280**, 14709–14715 (2005).

20. X. Cui, Y. Yu, S. Gupta, Y. M. Cho, S. P. Lees-Miller and K. Meek, Autophosphorylation of DNA-dependent protein kinase regulates DNA end processing and may also alter double-strand break repair pathway choice. *Mol. Cell. Biol.* **25**, 10842–10852 (2005).

21. Y. Ma, U. Pannicke, H. Lu, D. Niewolik, K. Schwarz and M. R. Lieber, The DNA-dependent protein kinase catalytic subunit phosphorylation sites in human Artemis. *J. Biol. Chem.* **280**, 33839–33846 (2005).

22. P. Douglas, X. Cui, W. D. Block, Y. Yu, S. Gupta, Q. Ding, R. Ye, N. Morrice, S. P. Lees-Miller and K. Meek, The DNA-dependent protein kinase catalytic subunit is phosphorylated *in vivo* on threonine 3950, a highly conserved amino acid in the protein kinase domain. *Mol. Cell. Biol.* **27**, 1581–1591 (2007).

23. S. T. Kim, D. S. Lim, C. E. Canman and M. B. Kastan, Substrate specificities and identification of putative substrates of ATM kinase family members. *J. Biol. Chem.* **274**, 37538–37543 (1999).

24. J. S. Bedford and W. C. Dewey, Historical and current highlights in radiation biology: has anything important been learned by irradiating cells? *Radiat. Res.* **158**, 251–291 (2002).

25. W. C. Dewey and J. S. Bedford, Radiobiologic principles. In *Textbook of Radiation Oncology* (S. A. Leibel and T. L. Phillips, Eds.), pp. 3–25. W. B. Saunders, Philadelphia, 1998.

26. W. C. Dewey and A. Cole, Effects of heterogeneous populations on radiation survival curves. *Nature* **194**, 660–662 (1962).

27. T. T. Puck, S. J. Cieciura and A. Robinson, Genetics of somatic mammalian cells. III. Long-term cultivation of euploid cells from human and animal subjects. *J. Exp. Med.* **108**, 945–956 (1958).

28. L. H. Thompson, S. Fong and K. Brookman, Validation of conditions for efficient detection of HPRT and APRT mutations in suspension-cultured Chinese hamster ovary cells. *Mutat. Res.* **74**, 21–36 (1980).

29. P. A. Jeggo, L. M. Kemp and R. Holliday, The application of the microbial "tooth-pick" technique to somatic cell genetics, and its use in the isolation of X-ray sensitive mutants of Chinese hamster ovary cells. *Biochimie* **64**, 713–715 (1982).

30. R. A. Tobey and K. D. Ley, Isoleucine-mediated regulation of genome repliction in various mammalian cell lines. *Cancer Res.* **31**, 46–51 (1971).

31. T. C. Hsu and O. Klatt, Mammalian chromosomes *in vitro*. IX. On genetic polymorphism in cell populations. *J. Natl. Cancer Inst.* **21**, 437–473 (1958).

32. K. Rothkamm, I. Kruger, L. H. Thompson and M. Lobrich, Pathways of DNA double-strand break repair during the mammalian cell cycle. *Mol. Cell. Biol.* **23**, 5706–5715 (2003).

33. H. Nagasawa, D. Fornace and J. B. Little, Induction of sister-chromatid exchanges by DNA-damaging agents and 12-O-tetradecanoyl-phorbol-13-acetate (TPA) in synchronous Chinese hamster ovary (CHO) cells. *Mutat. Res.* **107**, 315–327 (1983).

34. N. S. Verkaik, R. E. Esveldt-van Lange, D. van Heemst, H. T. Bruggenwirth, J. H. Hoeijmakers, M. Z. Zdzienicka and D. C. van Gent, Different types of V(D)J recombination and end-joining defects in DNA double-strand break repair mutant mammalian cells. *Eur. J. Immunol.* **32**, 701–709 (2002).

35. R. Parshad, K. K. Sanford and G. M. Jones, Chromatid damage after G_2 phase x-irradiation of cells from cancer-prone individuals implicates deficiency in DNA repair. *Proc. Natl. Acad. Sci. USA* **80**, 5612–5616 (1983).

36. R. Parshad, K. K. Sanford and G. M. Jones, Chromosomal radiosensitivity during the G_2 cell-cycle period of skin fibroblasts from individuals with familial cancer. *Proc. Natl. Acad. Sci. USA* **82**, 5400–5403 (1985).

37. H. Nagasawa and J. B. Little, Radiosensitivities of ten apparently normal human diploid fibroblast strains to cell killing, G_2-phase chromosomal aberrations, and cell cycle delay. *Cancer Res.* **48**, 4535–4538 (1988).

38. D. Scott, Chromosomal radiosensitivity and low penetrance predisposition to cancer. *Cytogenet. Genome Res.* **104**, 365–370 (2004).

39. J. M. Hinz, N. A. Yamada, E. P. Salazar, R. S. Tebbs and L. H. Thompson, Influence of double-strand-break repair pathways on radiosensitivity throughout the cell cycle in CHO cells. *DNA Repair (Amst.)* **4**, 782–792 (2005).

40. I. Kruger, K. Rothkamm and M. Lobrich, Enhanced fidelity for rejoining radiation-induced DNA double-strand breaks in the G_2 phase of Chinese hamster ovary cells. *Nucleic Acids Res.* **32**, 2677–2684 (2004).

41. P. Tamulevicius, M. Wang and G. Iliakis, Homology-directed repair is required for the development of radioresistance during S phase: interplay between double-strand break repair and checkpoint response. *Radiat. Res.* **167**, 1–11 (2007).

42. A. T. Natarajan, A. Berni, K. M. Marimuthu and F. Palitti, The type and yield of ionising radiation induced chromosomal aberrations depend on the efficiency of different DSB repair pathways in mammalian cells. *Mutat. Res.* **642**, 80–85 (2008).

43. C. H. Bassing, W. Swat and F. W. Alt, The mechanism and regulation of chromosomal V(D)J recombination. *Cell* **109** (Suppl.), S45–S55 (2002).

44. D. H. Buckley, R. E. Crowell, E. R. Heaphy, C. A. Stidley, J. F. Lechner, F. D. Gilliland and S. A. Belinsky, Reduced DNA-dependent protein kinase activity is associated with lung cancer. *Carcinogenesis* **22**, 723–727 (2001).

45. M. Sameya, K. Sakata, Y. Matsumoto, H. Yamamoto, M. Maruoka, H. Ikeda, K. Ando, Y. Hosoi, N. Suzuki and M. Hareyama, The association of DNA-dependent protein kinase activity with chromosomal instability and risk of cancer. *Carcinogenesis* **27**, 117–122 (2006).

46. H. S. Lee, G. Choe, K. U. Park, J. Park do, H. K. Yang, B. L. Lee and W. H. Kim, Altered expression of DNA-dependent protein kinase catalytic subunit (DNA-PKcs) during gastric carcinogenesis and its clinical implications on gastric cancer. *Int. J. Oncol.* **31**, 859–866 (2007).

47. X. Wang, C. Szabo, C. Qian, P. G. Amadio, S. N. Thibodeau, J. R. Cerhan, G. M. Petersen, W. Liu and F. J. Couch, Mutational analysis of thirty-two double-strand DNA break repair genes in breast and pancreatic cancers. *Cancer Res.* **68**, 971–975 (2008).

48. H. Nagasawa, J. R. Brogan, Y. Peng, J. B. Little and J. S. Bedford, Some unsolved problems and unresolved issues in radiation cytogenetics: a review and new data on roles of homologous recombination and non-homologous end joining. *Mutat. Res.* **701**, 12–22 (2010).

Animal Reproduction Science 122 (2010) 303–312

Contents lists available at ScienceDirect

Animal Reproduction Science

journal homepage: www.elsevier.com/locate/anireprosci

Aberrant CpG methylation of the imprinting control region KvDMR1 detected in assisted reproductive technology-produced calves and pathogenesis of large offspring syndrome

Noboru Hori[a,e,1], Makoto Nagai[a,1], Muneyuki Hirayama[b], Tomokazu Hirai[c], Keisuke Matsuda[d], Michiko Hayashi[a], Takaichi Tanaka[e], Tadashi Ozawa[f], Shin-ichi Horike[g,*]

[a] *Ishikawa Prefectural Livestock Research Center, Hodatsushimizu, Ishikawa 929-1325, Japan*
[b] *National Livestock Breeding Center, Nishi-shirakawa, Fukushima 961-8511, Japan*
[c] *National Livestock Breeding Center Tokachi station, Otohuke, Hokkaido 080-0572, Japan*
[d] *Matsuda Dairy Herd Service, Tsubata, Ishikawa 929-0327, Japan*
[e] *Ishikawa Nanbu Livestock Hygiene Service Center, Kanazawa, Ishikawa 920-3101, Japan*
[f] *Ishikawa Hokubu Livestock Hygiene Service Center, Nanao, Ishikawa 929-2126, Japan*
[g] *Frontier Science Organization, Institute for Gene Research, Kanazawa University, Kanazawa, Ishikawa 920-0934, Japan*

ARTICLE INFO

Article history:
Received 7 June 2010
Received in revised form
18 September 2010
Accepted 24 September 2010
Available online 7 October 2010

Keywords:
Genomic imprinting
In vitro fertilization
Somatic cell nuclear transfer
DNA methylation

ABSTRACT

Although somatic cell nuclear transfer (NT) and *in vitro* fertilization (IVF) have the potential to produce genetically superior livestock, considerable numbers of abnormally large animals, including sheep and cattle affected by "large offspring syndrome" (LOS), have been produced by these assisted reproductive technologies (ART). Interestingly, these phenotypes are reminiscent of Beckwith–Wiedemann syndrome (BWS) in humans, which is an imprinting disorder characterized by pre- and/or postnatal overgrowth. The imprinting control region KvDMR1, which regulates the coordinated expression of growth control genes such as *Cdkn1c*, is known to be aberrantly hypomethylated in BWS. Therefore, we hypothesized that aberrant imprinting in this region could contribute to LOS. In this study, we analyzed the DNA methylation status of the *Kcnq1ot1/Cdkn1c* and *Igf2/H19* domains on bovine chromosome 29 and examined the coordinated expression of imprinted genes surrounding them in seven calves derived by NT (which showed signs of developmental abnormality), two calves conceived by IVF (both developmentally abnormal), and three conventional calves that died of unrelated causes. Abnormal hypomethylation status at an imprinting control region of *Kcnq1ot1/Cdkn1c* domain was observed in two of seven NT-derived calves and one of two IVF-derived calves in almost all organs. Moreover, increased expression of *Kcnq1ot1* and diminished expression of *Cdkn1c* were observed by RT-PCR analysis. This study is the first to describe the abnormal hypomethylation of the KvDMR1 domain and subsequent changes in the gene expression of *Kcnq1ot1* and *Cdkn1c* in a subset of calves produced by ART. Our findings provide strong evidence for a role of altered imprinting control in the development of LOS in bovines.

1. Introduction

Assisted reproductive technologies (ART) such as nuclear transfer (NT) and *in vitro* fertilization (IVF) have been used to produce genetically superior livestock. How-

* Corresponding author. Tel.: +81 76 265 2775; fax: +81 76 234 4537.
E-mail address: sihorike@staff.kanazawa-u.ac.jp (S.-i. Horike).
[1] These authors contributed equally to this work.

0378-4320/$ – see front matter © 2010 Elsevier B.V. All rights reserved.
doi:10.1016/j.anireprosci.2010.09.008

ever, animals produced by ART techniques suffer from a higher frequency of various abnormalities including large size at birth, enlarged umbilical cord, and enlarged organs (Behboodi et al., 1995; Constant et al., 2006; Wilmut et al., 2002; Young et al., 1998). These alterations in phenotype, called "large offspring syndrome" (LOS), have not only been observed in cattle but also in sheep (Wilmut et al., 1997, 2002) and mice (Eggan et al., 2001; Fernández-Gonzalez et al., 2004; Wakayama et al., 1998) produced by ART techniques. These phenotypes are reminiscent of Beckwith–Wiedemann syndrome (BWS) (OMIM:130650) in humans, an overgrowth syndrome associated with congenital malformations and tumor predisposition (Amor and Halliday, 2008; DeBaun et al., 2003; Maher et al., 2003; Maher, 2005; Manipalviratn et al., 2009; Shiota and Yamada, 2005).The molecular basis of BWS is complex and heterogeneous. The syndrome is associated with epigenetic alterations at 1 of 2 imprinted domains on human chromosome 11p15.5, KvDMR1 and ICR1 (Enklaar et al., 2006; Ideraabdullah et al., 2008; Delaval et al., 2006; Smith et al., 2007; Weksberg et al., 2003, 2005). According to previous studies (Horike et al., 2000), KvDMR1 is associated with a paternally expressed untranslated RNA (*Kcnq1ot1*) and downregulation *in cis* of *Cdkn1c* expression. An alternative locus whose aberrant imprinting has been implicated in LOS is ICR1. ICR1 is associated with the expression of genes *Igf2* and *H19*, but not more centromic genes such as *Cdkn1c*. Several studies have shown that epigenetic alterations in the *Igf2/H19* domain are associated with LOS in cattle, sheep, and mice produced by ART techniques (Curchoe et al., 2009; DeChiara et al., 1991; Doherty et al., 2000; Khosla et al., 2001; Li et al., 2005; Moore et al., 2007; Yang et al., 2005; Young et al., 2003; Zhang et al., 2004). However, 50% of sporadic BWS cases show loss of CpG methylation at KvDMR1, which may function as a regional imprinting center on the *Kcnq1ot1/Cdkn1c* domain. Therefore, it is possible that LOS is related to the loss of CpG methylation at KvDMR1, leading to diminished expression of *Cdkn1c*.

Indeed, Couldrey and Lee (2010) have recently reported hypomethylation of KvDMR1 in mid-gestation bovine fetuses produced by NT. They have suggested that methylation levels at KvDMR1 might be associated with the variable overgrowth phenotypes seen in NT fetuses. However, it remains unknown whether hypomethylation at KvDMR1 is linked to the aberrant expression of *Kcnq1ot1*, *Cdkn1c*, *Igf2*, or *H19*. In this study, we analyzed the DNA methylation levels of the *Kcnq1ot1/Cdkn1c* and *Igf2/H19* domains on bovine chromosome 29 and examined the expression of *Kcnq1ot1*, *Cdkn1c*, *H19*, and *Igf2* in NT- and IVF-derived full-term calves. Here we show that loss of CpG methylation of KvDMR1 and aberrant gene expression of *Kcnq1ot1* and *Cdkn1c* may contribute to LOS in animals conceived using ART techniques.

2. Materials and methods

2.1. Collection and maturation of oocytes

Cow ovaries were obtained from a slaughterhouse and transported to the laboratory in physiological saline at 20 °C. Cumulus oocyte complexes (COCs) were recovered from ovaries by aspiration using disposable pumps. Groups of 20–40 were matured in a 100-μL drop of Tissue Culture Medium-199 (TCM199) (Invitrogen, Carlsbad, CA) with 5% calf serum (CS) covered with paraffin oil for 20 h in a humidified environment of 5% CO_2 in air at 38.5 °C.

2.2. Donor cells, NT, and embryo transfer

Adult ear fibroblast cells from Japanese black bull at passages 4–10 were used for NT. NT was performed according to the method described by Goto et al. (1999) with minor modifications. Briefly, metaphase II oocytes were stripped of cumulus cells by pipetting in phosphate-buffered saline (PBS) with 0.5% hyaluronidase (Sigma, St. Louis, MO). The zonae pellucidae of the oocytes were cut near the polar body and enucleated with a glass needle by pushing out the cytoplasm, including the nucleus, in PBS containing 20% CS and 5 μg/mL cytocharacin B (Sigma). Successful enucleation was verified by visualizing the polar body under UV light after staining with 5 μg/mL Hoechst 33342 (Sigma) in PBS. The adult ear fibroblast cells were prepared by trypsinization and resuspended in TCM199 with 5% CS. Single cells were transferred to the perivitelline space and electrically fused with one pulse of 25 V for 50 μs using a needle-type electrode in Zimmerman medium. The fused embryos were incubated in TCM199 with 5% CS and 10 μg/mL cycloheximide covered with paraffin oil for 6 h. After the activation treatments described above, the nuclear-transplant oocytes were cultured in CR1aa medium (Rosenkrans et al., 1993) with 5% CS under the same conditions used during oocyte maturation for 8 d. A single morphologically normal blastocyst developed to the blastocyst stage was transferred nonsurgically to the uterine horn of a synchronous recipient.

2.3. IVF

The IVF was essentially performed as described previously (Imai et al., 2006). Briefly, straws of commercially frozen sperm from a single Holstein bull were thawed in a water bath at 37 °C, layered on top of 3 mL 90% Percoll (Parrish et al., 1995), and centrifuged at 750 × *g* for 10 min. The top layer was discarded, spermatozoa were washed with Brackett and Oliphant (BO) medium (Brackett and Oliphant, 1975), and the concentration of spermatozoa was then adjusted to 3×10^6 spermatozoa/mL in BO medium containing 5 mM hypotaurine (Sigma), 2 U/mL heparin (Novo-Heparin Injection 1000; Aventis Pharma Ltd., Paris, France), and 10 mg/mL BSA (Sigma). Droplets of the spermatozoa suspension (100 μL) covered with paraffin oil were prepared, and approximately 20 oocytes matured *in vitro* were transferred to each droplet and incubated for 6 h. After insemination, presumptive zygotes were stripped of cumulus cells by pipetting, washed in CR1aa containing 5% CS, and cultured under the same conditions used during oocyte maturation for 7 d. Morphologically normal blastocysts developed to the early-blastocyst or blastocyst stage were transferred nonsurgically to the uterine horns of synchronous recipients.

Table 1
Symptom features of the clones and *IVF* calves used in this study.

Cattle no.	Breed	Sex	Body weight (kg)[a]	Over weight	Enlarged umbilical cord	Enlarged organ	Day of death
Clone-1	Japanese black	Male	48.0	+	+	–	1
Clone-2	Japanese black	Male	68.5	+	+	–	21
Clone-3	Japanese black	Male	62.0	+	+	+	2
Clone-4	Japanese black	Male	57.5	+	+	–	2
Clone-5	Japanese black	Male	51.0	+	+	–	219
Clone-6	Japanese black	Male	39.5	+	–	–	120
Clone-7	Japanese black	Male	45.0	+	–	–	5
IVF-1	Holstein	Female	60.0	+	+	–	5
IVF-2	Holstein	Female	60.0	+	+	–	1

[a] At birth (normal weight: Japanese black, 29.5 kg; Holstein, 45 kg (average weight of calves produced by artificial insemination or embryo transfer at National Livestock Breeding Center, Tokachi station)).

2.4. Calves produced by NT or IVF and preparation of genomic DNA

Production of NT or IVF calves was carried out according to the Guide for Care and Use of Experimental Animals at the National Livestock Breeding Center and the Fundamental Guidelines for Proper Conduct of Animal Experiments and Related Activities in Academic Research Institutions under the jurisdiction of the Ministry of Education, Culture, Sports, Science and Technology of Japan. Nine calves, i.e., seven derived by NT (clones-1, -2, -3, -4, -5, -6, and -7) and two by IVF (IVF-1 and 2), were used in this study. All animals died or were slaughtered due to musculoskeletal abnormalities within 219 d after the perinatal period. Individual clinical characteristics are listed in Table 1. Three animals produced by conventional breeding that died within 163 d after birth due to accidents or diarrhea were used as controls (normal-1, -2, and -3). Lung, heart, liver, kidney, and spleen samples were recovered from each calf. All tissues were collected immediately after death. Genomic DNA from organ samples of NT, IVF, and conventional calves was extracted using Wizard® Genomic DNA Purification Kit (Promega, Valencia, CA) according to the manufacturer's instructions.

2.5. DNA methylation analysis by HpaII–MspI–McrBC PCR assay

Chromosome 29 of *Bos taurus* contains an imprinted chromosomal region orthologous to the human 11p15.5 region and mouse distal chromosome 7, a 1-Mb cluster of evolutionarily conserved imprinted genes with two imprinting control regions (ICR1 and KvDMR1) (Beatty et al., 2006; Horike et al., 2000, 2009). Sequences of bovine *Kcnq1ot1*, *Cdkn1c*, *Igf2*, and *H19* on chr 29 were predicted using the UCSC Genome Browser (http://genome.ucsc.edu) (Fig. 1A). Primer pairs for the HpaII–MspI–McrBC PCR assay were designed in the *Cdkn1c* promoter region, KvDMR1, and ICR1 (Fig. 1B and C) using Primer3 software (http://frodo.wi.mit.edu/primer3). The sequences of primers were as follows: *Cdkn1c* promoter forward primer 5′-CCTTGCAGACAAAGGAGCTG-3′ and reverse primer 5′-GACTGCTCCTGAGGCTCGTT-3′; KvDMR1 forward primer 5′-GTCTGGGCTCACAGTGCTC-3′ and reverse primer 5′-GTGGACTCAGCTACGCGACT-3′; and ICR1 forward primer 5′-AGGCTCACACATCACCACAA-3′ and reverse primer 5′-AGGCTCAGATGAGTGCCTGT-3′.

Genomic DNA (3 μg) was digested with 30 U HpaII, MspI, or McrBC overnight at 37 °C in 100 μL of reaction mixture following the instructions of the manufacturer (HpaII, MspI and McrBC; New England Biolabs Inc., Massachusetts, USA.). After incubation, digested samples were purified by phenol–chloroform extraction and ethanol precipitation and dissolved in distilled water. For PCR, 1.0 μL (50 ng) of digested genomic DNA was used in a 20-μL PCR reaction solution. PCR was performed using GoTaq® Master Mix (Promega) for KvDMR1 and ICR1, or KOD FX (Toyobo, Osaka, Japan) for *Cdkn1c* promoter. For KvDMR1 and ICR1, we repeated all reactions at least three times with the following PCR cycling protocol: 2 min heat start at 95 °C and 29 cycles of denaturation at 95 °C for 30 s, annealing at 58 °C for 30 s, and extension at 72 °C for 1 min. For the *Cdkn1c* promoter, cycling protocol consisted of 2 min heat start at 94 °C and 30 cycles of denaturation at 98 °C for 10 s, annealing and extension at 68 °C for 1 min.

2.6. DNA methylation analysis by bisulfite sequencing

Bisulfite conversion of genomic DNA and purification of modified DNA was conducted using EpiTect® Bisulfite Kits (Qiagen, Hilden, Germany) according to manufacturer's instructions. Specific primers for the amplification of bisulfite-treated DNA were designed at the regions consistent with HpaII–MspI–McrBC PCR assay (Fig. 1B and C) using MethPrimer (http://www.urogene.org/methprimer) as follows: KvDMR1 forward primer 5′-TTGGATTTGTGTTTGGAGGTTAT-3′ and reverse primer 5′-AACTCAAAATTTCCACTACACCTAAAA-3′; ICR1 forward primer 5′-TTTTAGATAGGGTTGAGAGGTTGTG-3′ and reverse primer 5′-AACCCTATAAACCACTATAATATCC-3′. PCR was performed using GoTaq® Master Mix (Promega). PCR conditions were as follows: 2 min heat start at 95 °C and 32 cycles of denaturation at 95 °C for 30 s, annealing at 58 °C for 30 s, and extension at 72 °C for 30 s. The PCR products were directly cloned into the pGEM®-T Easy vector (Promega). Twenty individual clones were sequenced from both ends using a 310 Genomic Analyzer (Applied Biosystems Inc., Foster City, CA) according to the standard protocol. In order to evaluate the differences

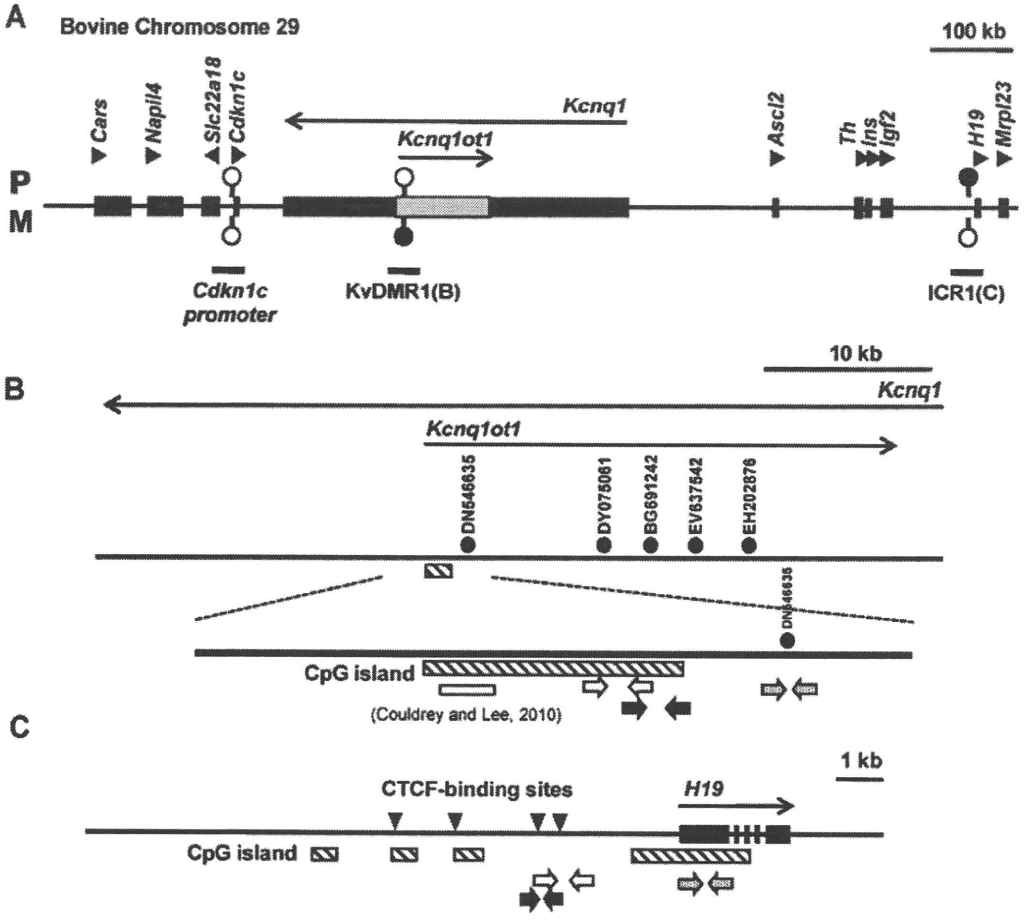

Fig. 1. Methylation analyses of chromosome 29 in cattle produced by NT, IVF and normal reproduction. A: Physical map of the imprinted cluster in bovine chromosome 29. Previously identified genes or transcripts (boxes) are drawn approximately to scale. Transcriptional orientation is indicated by arrows and arrowheads. Open circles indicate unmethylated CpG sites and filled circles indicate methylated CpG sites. We examined the DNA methylation status of the *Cdkn1c* promoter, ICR1, and KvDMR1 using HpaII–MspI–McrBC PCR assays. B: Bovine KvDMR1, with five ESTs indicated by filled circles. The primers used for HpaII–MspI–McrBC PCR, bisulfite modification PCR, and RT-PCR are indicated by open, filled, and spotted arrows, respectively. The genomic region analyzed by Couldrey and Lee (2010) is indicated by an open box. C: The ICR1 domain upstream of *H19*. The filled triangles indicate putative CTCF-binding sites. The primers used for HpaII–MspI–McrBC PCR, bisulfite modification PCR, and RT-PCR are indicated by open, filled, and spotted arrows, respectively.

in the CpG methylation density (methylated CpGs/total CpGs) between normal and ART calves, a comparative statistical analysis was performed. Arcsine transformation was applied for the values of CpG methylation density. The mean and 95% confidence interval of the transformed values from three normal calves was calculated. The values from NT and IVF calves were compared to those from normal calves and any values above or below the 95% confidence intervals were considered to be statistically significant.

2.7. RT-PCR analysis

Total RNA was extracted using TriPure Isolation Reagent (Roche, Mannheim, Germany) according to the manufacturer's instructions. To remove any possible contamination of gDNA, the total RNA was treated with RNase-free DNase I (Takara, Shiga, Japan). First strand cDNA synthesis was carried out using the PrimeScript II 1st strand cDNA Synthesis Kit (Takara) according to manufacturer's instructions. For expression analysis of *Kcnq1ot1*, *Cdkn1c*, *Igf2*, and *H19*, RT-PCR analysis was performed by using GoTaq® Master Mix (Promega). We repeated all reactions at least three times with the following cycling protocol: 2 min heat start at 95 °C and 35 cycles of denaturation at 95 °C for 30 s, annealing at 55 °C for 30 s, and extension at 72 °C for 30 s. Gene-specific primers were designed from bovine EST sequence data (Table 2). All primers were designed to encompass at least one intron, with the exception of *Kcnq1ot1*. The imprinting analysis of *Kcnq1ot1* in normal crossbred cattle (Japanese black X Holstein) was performed using the forward primer 5′-TTGCTATGTTCCTCCCTGCT-3′ and the reverse primer 5′-ACCCCCATCTCTACCCTGAA-3′. The imprinting analysis of *Kcnq1ot1* in IVF-2 was performed using the forward primer 5′-CGAGAATGGGAGGAGAGTCA-3′ and the reverse primer 5′-ACACCACACACTCACCCTGA-3′. The PCR product was then directly sequenced using the 310 Genomic Analyzer.

Table 2
Primer sequences, GenBank accession numbers, and RT-PCR product size.

	Sequence (5′ → 3′)	GenBank accession no.	Product size (bp)
Cdkn1c	Forward: GCC TCT CAT CTC CGA CTT CTT Reverse: CAG TGT ACT CCT TGG GCA GA	BC123620	355
Kcnq1ot1	Forward: GAAGGCCTTGTACCAGCAGA Reverse: CCGGGTCCTGAATAAGATCC	DN546635	340
Igf2	Forward: ACCCTCCAGTTTGTCTGTGG Reverse: GGTGACTCTTGGCCTCTCTG	BC126514	349
H19	Forward: TGA TAT GGT CCG GTG TGA TG Reverse: CGT CCG TTC CTT TAG GTC AA	CN433427	320
Gapdh	Forward: ACC CAG AAG ACT GTG GAT GG Reverse: CCC AGC ATC GAA GGT AGA AG	DV778924	345

3. Results

3.1. Methylation status of the promoter region of Cdkn1c, ICR1, and KvDMR1 in NT, IVF, and normal calves

The imprinting control region KvDMR1 is known to be aberrantly hypomethylated in BWS, which shows features akin to those of LOS, and therefore aberrant imprinting in this region could contribute to LOS. We examined the DNA methylation status of the *Cdkn1c* promoter, ICR1, and KvDMR1 using HpaII–MspI–McrBC PCR assays (Fig. 1). Digestion profiles were visualized by PCR amplification. HpaII and MspI recognize the CCGG sequence, but HpaII digestion is inhibited by CpG methylation at the internal cytosine while MspI is not. McrBC cleaves DNA containing a methylated cytosine and does not act upon unmethylated DNA (Fiona et al., 2000; Panne et al., 1999). In the case of a fully methylated sequence, amplification would be obtained only from the HpaII-digested template. In contrast, an unmethylated sequence is digested only with HpaII but not with McrBC, and hence amplification would be obtained only from the McrBC-digested DNA. If the target sequence is differentially methylated, such as the imprinting control region, amplification will be obtained from both HpaII- and McrBC-digested DNA. We employed these enzymes to screen DNA methylation status in lung, heart, liver, kidney, and spleen samples from NT, IVF, and normal calves. For the *Cdkn1c* promoter, amplification was obtained only from the McrBC-digested DNA, as indicating that both maternal and paternal alleles are unmethylated (data not shown). For KvDMR1, clone-3 (except the spleen), clone-5, and IVF-2 (except the liver) displayed diminished amplification from HpaII-digested DNA; all other samples demonstrated differentially methylated status (Fig. 2A). Thus, the HpaII–MspI–McrBC PCR assays revealed aberrant KvDMR1 hypomethylation in clone-3, clone-5, IVF-2, although comparable amplification from HpaII- and McrBC-digested DNA was observed in some organs (data not shown). For ICR1, amplification was obtained from both HpaII- and McrBC-digested DNA from all samples, indicating that this region is differentially methylated (Fig. 3A).

We further confirmed the results obtained from the HpaII–MspI–McrBC PCR assays by bisulfite sequencing analysis. Treatment of DNA with sodium bisulfite leads to the conversion of unmethylated cytosine, but not 5-methyl cytosine, to uracil. Following PCR amplification of KvDMR1 and ICR1 from bisulfite-treated DNA, the PCR products were cloned into the pGEM®-T Easy vector and individually sequenced. The CpG methylation density of KvDMR1 in lung samples from normal-1 (49.8%, 199/400), -2 (47.0%, 79/168), and -3 (45.8%, 103/225) was consistent with the HpaII–MspI–McrBC PCR results. The CpG methylation density of KvDMR1 in clone-3 (11.6%, 58/500), clone-5 (23.0%, 109/475), and IVF-2 (32.2%, 228/708) were low compared with those of control, also confirming the HpaII–MspI–McrBC PCR results (Fig. 2A, Table 3). The arcsine-transformed values of clone-3 (0.116), clone-5 (0.23), and IVF-2 (0.332) were below the confidence interval of the transformed values from the three normal calves (0.437–0.554). Thus, these methylation densities were considered to be significantly lower than those of controls. In addition, we identified a single nucleotide polymorphism (SNP) at KvDMR1 in IVF-2, enabling us to distinguish between parental alleles at KvDMR1. Bisulfite sequencing confirmed that the methylated allele (allele1: perhaps the maternal allele, Fig. 2B) is specifically demethylated in IVF-2, indicating aberrant hypomethylation status. The KvDMR1 methylation densities of clones-1, -2, -4, -6, -7 and IVF-1 were 45.4% (227/500), 52.8% (264/500), 74.0% (296/400), 54.0% (270/500), 66.3% (348/525), and 44.4% (79/168), respectively (data not shown). For ICR1, although HpaII–MspI–McrBC PCR demonstrated that the amount of PCR products obtained from HpaII- and McrBC-digested DNA were almost equal, bisulfite sequencing demonstrated a hypermethylation trend in the CpG methylation density of lung samples from normal-1 (66.2%; 176/266), clone-3 (65.4%, 170/266), -5 (70.7%, 198/280), and IVF-2 (69.9%, 380/546) (Fig. 3B). However, the CpG methylation densities of ICR1 in normal-2 and normal-3 were also 77.4% (412/532) and 63.1% (159/252), respectively (data not shown). Since the arcsine-transformed values of clone-3 (0.713), clone-5 (0.785), and IVF-2 (0.774) were within the confidence interval of the transformed values from the three normal calves (0.498–1.02), these hypermethylation trends were considered normal. Therefore, these hypermethylation trends were due to bias in the bisulfate sequencing assay, as reported previously (Curchoe et al., 2009; Kremenskoy et al., 2006). Finally, we concluded that there are no differences in the CpG methylation pattern at ICR1 among NT, IVF, and control animals.

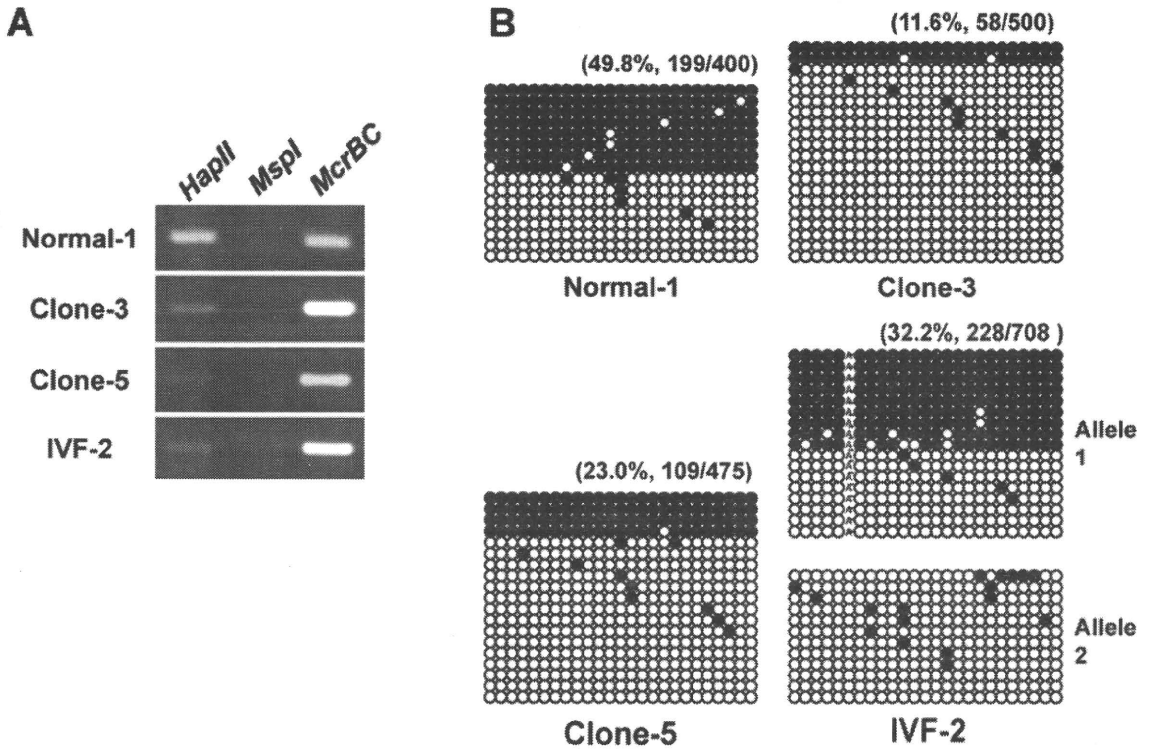

Fig. 2. DNA methylation status of KvDMR1 in lung samples from NT, IVF and normal cattle. A: DNA methylation status of KvDMR1 using HpaII–MspI–McrBC PCR assays. B: Methylation profiles of 25 CpG dinucleotides of KvDMR1. Each circle indicates a CpG site in the primary DNA sequence, and each line of circles represents analysis of a single cloned allele. Filled circles represent methylated CpGs, and open circles represent unmethylated sites. Scores for the methylation of each CpG were obtained by sequencing PCR clones derived from bisulfite-treated genomic DNA. "A" in IVF-2 indicates G/A SNPs.

3.2. Expression analysis of Kcnq1ot1, Cdkn1c, H19, and Igf2 genes in clone-3, 5, IVF-2 calves

To determine whether hypomethylation at KvDMR1 was linked to the aberrant expression of *Kcnq1ot1*, *Cdkn1c*, *Igf2*, or *H19*, we performed RT-PCR analysis on lung and kidney samples from clone-3, -5, and IVF-2, and compared gene expression patterns with those of a normal calf. The expression of *Gapdh* was used as a control. We examined the expression of *Kcnq1ot1* transcripts defined by five expressed sequence tags (ESTs) across the 60-kb *Kcnq1ot1* locus (Fig. 1). In comparison to the normal calf, *Kcnq1ot1* transcript levels were increased in clone-3, -5, and IVF-2, whereas the *Cdkn1c* transcript levels were reduced. No significant differences between clone-3, 5, or IVF-2 and the normal calf were detected in *H19* or *Igf2* expression (Fig. 4, Table 3). We also examined the imprinted expression of *Kcnq1ot1* in lung tissue from normal cattle and IVF-2 by using SNPs, enabling us to distinguish between parental alleles of expressed *Kcnq1ot1* (Fig. 5). The imprinting analysis confirmed that bovine *Kcnq1ot1* transcripts are monoallelically expressed in normal lung tissue. In IVF-2, the *Kcnq1ot1* transcripts were biallelically expressed, consistent with the aberrant CpG methylation of KvDMR1.

Table 3
Summary of KvDMR1 methylation analysis and imprinted expression in NT, IVF, and normal cattle.

	Clone-1	Clone-2	Clone-3	Clone-4	Clone-5	Clone-6	Clone-7	IVF-1	IVF-2	Normal-1	Normal-2	Normal-3
Methylation (lung)												
Signs of developmental abnormality	+	+	+	+	+	+	+	+	+	–	–	–
HpaII–MspI–McrBC assay	DM[a]	DM	Hypo[b]	DM	Hypo	DM	DM	DM	Hypo	DM	DM	DM
Bisulfite sequence assay (%)	45.4	52.8	11.6	74.0	23.0	54.0	66.3	44.4	32.2	49.8	47.0	45.8
Expression (lung and kidney)												
H19	♦	♦	♦	♦	♦	♦	♦	♦	♦	♦	♦	♦
Igf2	♦	♦	♦	♦	♦	♦	♦	♦	♦	♦	♦	♦
Kcnq1ot1	♦	♦	↑↑	♦	↑↑	♦	♦	♦	↑↑[c]	♦	♦	♦
Cdkn1c	♦	♦	↓↓↓	♦	↓↓	♦	♦	♦	↓↓	♦	♦	♦

[a] Differentially methylated.
[b] Hypomethylated.
[c] Biallelic expression, ♦ no change, ↑ upregulated, ↓ downregulated.

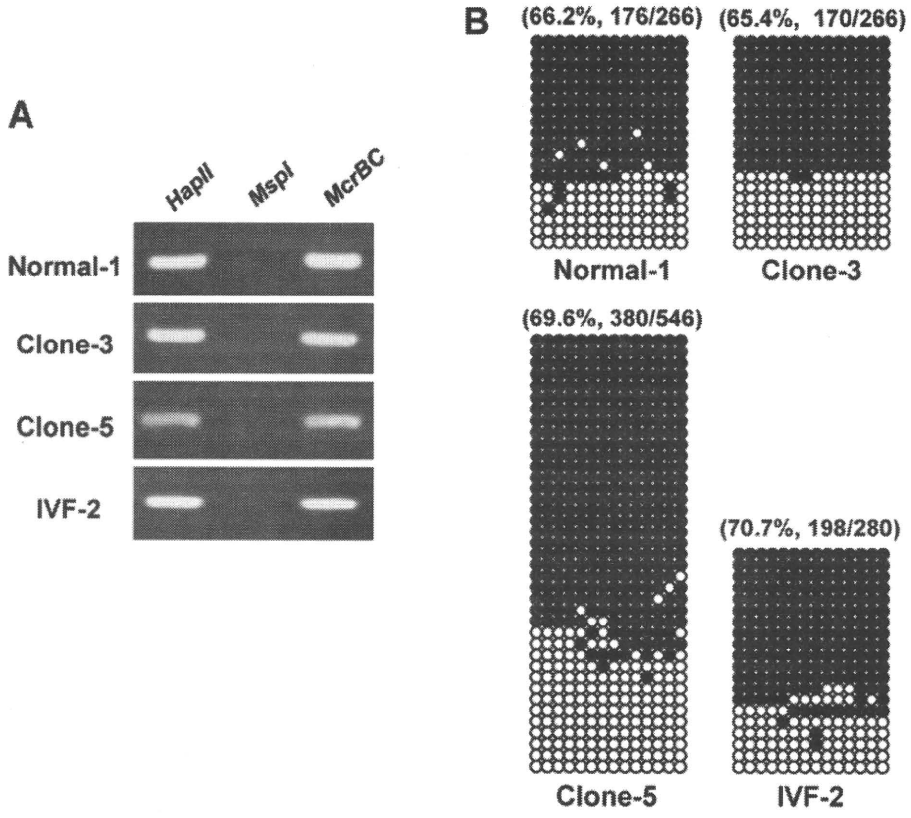

Fig. 3. DNA methylation status of ICR1 in lung samples from NT, IVF and normal cattle. A: DNA methylation status of ICR1 using HpaII–MspI–McrBC PCR assays. B: Methylation profiles of 14 CpG dinucleotides of ICR1. Filled circles represent methylated CpGs, and open circles represent unmethylated sites. Scores for the methylation of each CpG were obtained by sequencing PCR clones derived from bisulfite-treated genomic DNA.

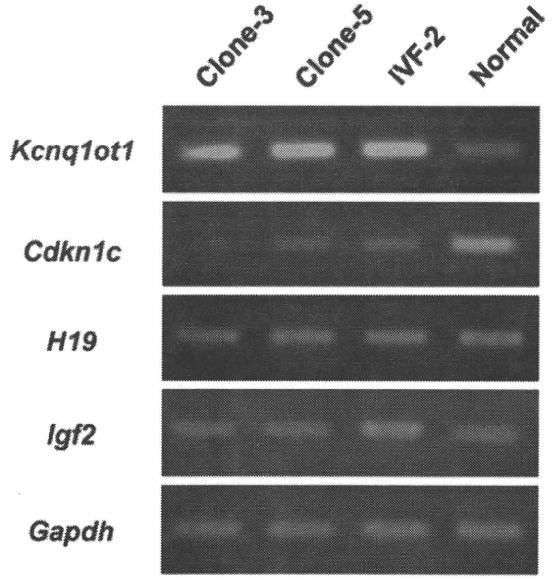

Fig. 4. RT-PCR analysis of *Kcnq1ot1*, *Cdkn1c*, *H19*, and *Igf2* genes in the lung and kidney tissues from clone-3, clone-5, and IVF-2. *Gapdh* was used as a control. No amplification was detected from negative control templates and reverse transcriptase minus mock-cDNA reactions (data not shown).

4. Discussion

Imprinted genes are expressed in a mono-allelic manner, which is inherited either maternally or paternally. This phenomenon is a particularly important epigenetic mechanism in mammals, and is thought to influence fetal and placental growth and development (Abu-Amero et al., 2006; Angiolini et al., 2006; Coan et al., 2005; Fowden et al., 2006; Hitchins and Moore, 2002). Aberrant imprinting disturbs development and is the cause of various developmental disorders, including BWS, Russell–Silver syndrome, and Prader–Willi/Angelman syndrome in humans (Enklaar et al., 2006; Horike et al., 2009; Horsthemke and Wagstaff, 2008; Weksberg et al., 2003, 2005). Recently, an association between ART techniques and aberrant imprinting has been recognized in humans and mice (Amor and Halliday, 2008; DeBaun et al., 2003; Maher et al., 2003; Maher, 2005; Manipalviratn et al., 2009; Shiota and Yamada, 2005, 2009). In cattle and sheep, few reports to date have described the aberrant expression of imprinted genes in LOS animals produced by ART techniques. In this study, to test if disorders, such as LOS, that are more frequent in ART-conceived cattle are caused by epigenetic alterations, we investigated the CpG methylation status and expression of *Kcnq1ot1*, *Cdkn1c*, *Igf2*, and *H19* in calves produced by ART techniques.